Received: 22 July 2023 | Revised: 10 November 2023 | Accepted: 1 January 2024

DOI: 10.1002/cbin.12129

RESEARCH ARTICLE

Cell Biology International WILEY

Endolysosomal two-pore channel 2 plays opposing roles in primary and metastatic malignant melanoma cells

Samantha Barbonari[1] | Antonella D'Amore[2] | Ali A. Hanbashi[2,3] | Fioretta Palombi[1] | Anna Riccioli[1] | John Parrington[2] | Antonio Filippini[1]

[1]Department of Anatomy, Histology, Forensic Medicine and Orthopedics, Unit of Histology and Medical Embryology, Sapienza University, Rome, Italy

[2]Department of Pharmacology, University of Oxford, Oxford, UK

[3]Department of Pharmacology, College of Pharmacy, Jazan University, Jazan, Saudi Arabia

Correspondence

Antonio Filippini, Department of Anatomy, Histology, Forensic Medicine and Orthopedics, Unit of Histology and Medical Embryology, Sapienza University, 16 Via A. Scarpa, 00161 Rome, Italy.
Email: antonio.filippini@uniroma1.it

John Parrington, Department of Pharmacology, University of Oxford, Mansfield Rd, Oxford OX1 3QT, UK.
Email: john.parrington@worc.ox.ac.uk

Funding information

Sapienza Università di Roma, Grant/Award Number: B87G22001200001

Abstract

The ion channel two-pore channel 2 (TPC2), localised on the membranes of acidic organelles such as endo-lysosomes and melanosomes, has been shown to play a role in pathologies including cancer, and it is differently expressed in primary versus metastatic melanoma cells. Whether TPC2 plays a pro- or anti-oncogenic role in different tumour conditions is a relevant open question which we have explored in melanoma at different stages of tumour progression. The behaviour of primary melanoma cell line B16F0 and its metastatic subline B16F10 were compared in response to TPC2 modulation by silencing (by small interfering RNA), knock-out (by CRISPR/Cas9) and overexpression (by mCherry-TPC2 transfected plasmid). TPC2 silencing increased cell migration, epithelial-to-mesenchymal transition and autophagy in the metastatic samples, but abated them in the silenced primary ones. Interestingly, while TPC2 inactivation failed to affect markers of proliferation in both samples, it strongly enhanced the migratory behaviour of the metastatic cells, again suggesting that in the more aggressive phenotype TPC2 plays a specific antimetastatic role. In line with this, overexpression of TPC2 in B16F10 cells resulted in phenotype rescue, that is, a decrease in migratory ability, thus collectively resuming traits of the B16F0 primary cell line. Our research shows a novel role of TPC2 in melanoma cells that is intriguingly different in initial versus late stages of cancer progression.

KEYWORDS

cancer progression, cisplatin sensitivity, epithelial-to-mesenchymal transition, lysosomal calcium channels, TPC2

1 | INTRODUCTION

TPC2, a member of the ubiquitous two-pore channel family, is a sodium/calcium channel present on the membrane of acidic organelles such as endosomes, lysosomes and melanosomes (lysosome-related organelles) (Ambrosio et al., 2016). It is conserved from invertebrates to humans and has been shown to control diverse physiological functions (Webb et al., 2020), that include fertilization, neuromuscular differentiation, osteoclastogenesis, pancreatic acinar secretion and skin pigmentation (Bellono et al., 2016). At the cellular level, TPC2 has been shown to

John Parrington and Antonio Filippini share senior authorship, and are co-corresponding authors.

control basic functions such as autophagy and vesicular trafficking (Kondratskyi et al., 2018; Sun & Yue, 2018), the latter being shown to be involved in infections by viruses (Chao et al., 2023; Chen et al., 2022) such as Ebola virus (Sakurai et al., 2015), SARS-CoV, SARS-CoV-2 (Clementi et al., 2021) and MERS-CoV (Gunaratne et al., 2018). Evidence for TPC2 roles in mammalian pathology has been accumulating, showing its involvement in Parkinson's disease (Krogsaeter et al., 2022), neoangiogenesis (Favia et al., 2014, 2016; Minicozzi et al., 2023; Pafumi et al., 2017) and a number of cancers (Barbonari et al., 2022), including breast cancer (Nguyen et al., 2017), hepatocellular carcinoma (HCC) (Müller et al., 2021), leukaemia (Geisslinger et al., 2022) and malignant melanoma (D'Amore et al., 2020). The pigment-producing melanocyte is a cell type particularly rich in TPC2, which is expressed on the membrane of its melanin-containing acidic organelles, the melanosomes. TPC2 plays a role in skin and hair pigmentation, mediating changes from black/brown to blond colour, through modification of the pH and the size of the melanosomes, which control the production of melanin in melanocytes (Chao et al., 2017). Melanin pigments are also regulated in melanoma tumour cells, such as in the MNT-1 cell line, in which the knock-out and the overexpression of this channel is correlated with different amounts of melanin content. In particular, in MNT-1 cells the expression of TPC2 is inversely correlated with the production of melanin (Ambrosio et al., 2016). Lin-Moshier et al. have demonstrated that the interactome of TPC2 is specific for this channel and it is correlated with Ca^{2+} homeostasis, membrane organisation, the autophagic pathway, and cellular trafficking (Lin-Moshier et al., 2014). Until recently, the identity of the endogenous agonist of TPC2 as well as the biophysical characteristics and regulation of the channel have been a matter of debate. In particular there have been contrasting views on its preferential activation by nicotinic acid adenine dinucleotide phosphate (NAADP) (Ruas et al., 2015), or rather by phosphatidylinositol 3,5-bisphosphate (PI(3,5)P_2) (She et al., 2019) with different current activation (Ca^{2+} and Na^{+}) and biological effects reviewed in Patel et al. (2022). It has been recently demonstrated that TPC2 is bifunctional and displays differential ion selectivity depending upon the different activating ligand and agonist used (Gerndt et al., 2020; Saito et al., 2023). In particular, its P site is activated by PI(3,5)P_2 and is Na^{+} selective, while the N site is activated by NAADP and is Ca^{2+} selective. Moreover, the link between NAADP and TPC2 is not direct, but mediated by JPT2/HN1L and LSM12 (Gunaratne et al., 2021, 2023; Roggenkamp et al., 2021; Zhang et al., 2021). Interestingly, a number of new TPC2 activators and inhibitors have been described (Du et al., 2022; Gerndt et al., 2020; Minicozzi et al., 2023; Müller et al., 2021; Netcharoensirisuk et al., 2021; Pafumi et al., 2017). The unique features of the TPC2 channel have stimulated investigation into its role in the control of cell function, with the ultimate aim of targeting TPC2 therapeutically during clinical treatment (Jaślan et al., 2023; Skelding et al., 2022). The role of TPC2 in cancer has only recently begun to be investigated, with experimental evidence underscoring its potential significance in various malignancies reviewed in Alharbi and Parrington (2019, 2021a, 2021b) and Barbonari et al. (2022). To date, the evidence from different cellular models raises the question of whether TPC2 activation plays a pro- or anti-oncogenic role, because the modulation of this channel has been reported to result in different outcomes in different cancer cell lines. Of note, in MTN-1 melanoma cells, 4T1 murine breast cancer cells, hepatocellular carcinoma (HCC) cells, and T24 bladder cancer cells, the inhibition of TPC2 is correlated with reduced migration and invasiveness (Müller et al., 2021; Netcharoensirisuk et al., 2021; Nguyen et al., 2017), while in CHL1 melanoma cells, the inhibition of the same channel is correlated with increased metastatic traits (D'Amore et al., 2020). Moreover, in patients with bladder cancer, TPC2 upregulation correlates with an increase in patient survival (Shivakumar et al., 2017). Malignant melanoma (MM), a tumour of neuroectodermal origin arising from pigment-producing cells, melanocytes, is a deadly tumour and the sixth most common tumour type in Europe (Ferlay et al., 2021). It has been demonstrated that TPC2 has a differential expression between metastatic and primary patients in the Skin Cutaneous Melanoma data set analysis from TGCA (D'Amore et al., 2020), and this led us toask whether TPC2's differential expression may impact on cancer aggressiveness. To address this point we have made use of a common in vitro model, the B16 murine melanoma cell line, to comparatively explore the role of TPC2 in the primary (B16F0) line and in its more aggressive metastatic (B16F10) subline, obtained (Nicolson et al., 1978) by selecting cells for their ability to colonize the lung after intravenous injection. Here, we report how differently the two cell populations are affected by TPC2 knock-down, knock-out, or over-expression, in terms of parameters of aggressiveness, in particular migratory ability. These data show that within the same genetic background, TPC2 can play an opposing role at the late stages of cancer development, compared to the initial stages of carcinogenesis.

2 | MATERIALS AND METHODS

2.1 | Cells culture and reagents

B16F0 and B16F10 murine melanoma cells (ATCC-CRL-6322; CRL-6475) were cultured in Dulbecco's Modified Eagle Medium (DMEM) supplemented by 10% fetal bovine serum (FBS), 2% P/S and 2% L-glutamine (Sigma). Both cell lines were maintained at 37°C in a humidified 5% CO_2 incubator. Reagents used are: TPC2 siRNA (used at 10 nM, Cat. No. 1027415; Qiagen); Scramble siRNA (used at 10 nM; Bio-Fab research); Lipofectamine RNAiMAX (Thermofisher); Lipofectamine 2000 (Thermofisher); Cisplatin (Sigma). BafilomycinA1 (Sigma) is used in the last 3 h of the experiment at 100 nM.

2.2 | Western blot analysis

Total protein extraction of B16F0 and B16F10 cells was performed by homogenizing cells in lysis buffer containing protease and phosphatase inhibitor cocktail (Cell Signalling). The homogenates, after sonication, were centrifuged at 300*g* for 15 min at 4°C. Protein concentration was determined with a bicinchoninic acid assay (BCA) (Pierce). Protein lysates obtained from B16F0 and B16F10 cells were separated on sodium dodecyl sulfate–polyacrylamide gel electrophoresis gels and transferred on nitrocellulose membranes (Amersham Bioscience), which were

saturated with 5% nonfat dry milk in T-TBS. Then, membranes were incubated with primary antibodies overnight at 4° C and subsequently with peroxidase-conjugated secondary antibody (Jackson Laboratories). Antibody detection was performed by ECL (Cyanagen) and visualised by Chemidoc images. The intensity of western blot bands was quantified by ImageJ. Primary antibodies, diluted according to the manufacturer's instruction, were as follows: anti-LC3 (#2775; Cell Signalling), anti-AKT (#9272; Cell Signalling), anti-pAKT (s743) (#9271; Cell Signalling), anti-vimentin (Santacruz Biotch, Dallas, TX, USA sc-6260), anti-E-cadherin (#3195; Cell Signalling), anti-N-cadherin (#8203; Abcam), anti-PCNA (#2426; Abcam), anti-BCL2 (sc-492; Santacruz Biotch), anti-BAX (sc-493; Santacruz Biotch), and anti-Fascin1 (D-10, sc-46675; Santacruz Biotch). Normalisation was performed using horseradish peroxidase-conjugated β-actin (Sigma).

2.3 | Transient transfection of siRNA targeting mouse TPC2 and TPC2-mcherry plasmid

Lipofectamine RNAiMAX (Invitrogen) was used to transfect the cells with TPC2 siRNA. To facilitate transfection, the cells were incubated in 10% FBS containing DMEM; subsequently, they were plated to 80% confluence on a 12-well plate during transfection. The following day, we replaced the culture medium with 800 µL of Opti-MEM (ref #2342245; Gibco), which we then subjected to transfection using 2 µL of RNAiMAX. We mixed 100 µL of Opti-MEM and 2 µL of RNAiMAX and subjected the mixture to incubation for 5 min at room temperature. In another tube, 100 pM TPC2 siRNA or scrambled siRNA and 100 µL of Opti-MEM were combined. Subsequently, we added siRNA solution to the diluted RNAiMAX reagent, and the prepared 200-µL siRNA/RNAiMAX mixtures underwent incubation at room temperature for 25 min to facilitate the formation of the complex. Afterward, the cells and solution were combined. They together represented a final transfection volume of 1 mL. After 6-h incubation, 1 mL of standard growth medium was used to replace the transfection medium, which subsequently underwent culturing at 37°C. Lipofectamine 2000 (Thermofisher) was used to transfect the cells with TPC2-mcherry plasmid and empty-mCherry plasmid (TPC2-mCherry was a gift from Margarida Ruas (Addgene plasmid # 135183; http://n2t.net/addgene:135183; RRID:Addgene_135183; the empty plasmid was a gift from Federica Barbagallo, were used at 1000 ng/mL) based on the manufacturer's protocol.

2.4 | RNA extraction and quantitative real-time polymerase chain reaction (PCR)

Total RNA was extracted using TRIzol reagent (Invitrogen). Two micrograms of total RNA were used for complementary DNA (cDNA) synthesis; cDNA was synthesised from RNA using a high-capacity cDNA Reverse Transcription kit (Applied Biosystems), and real-time PCR was carried out using a power up SYBR green master mix (Applied Biosystems). Reactions were run in triplicate in three independent experiments. The geometric mean of the housekeeping

TABLE 1 List of primers used for gene expression analysis.

Gene	Primers
β-ActinFw	5′-TGACAGGATGCAGAA-3′
β-ActinRev	5′-GTACTTGCGCTCAGGAGGAG-3′
TPC2 Fw	5′-CCCCTGAGTTAGTTGGGGTGA-3′
TPC2 Rev	5′-CTGGAACTCATCAGCCAGCA-3′.

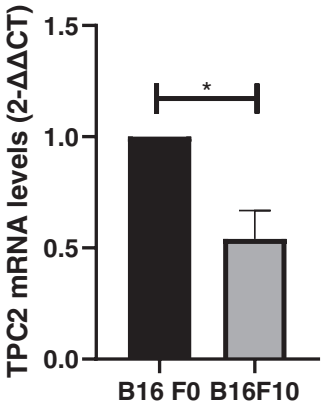

FIGURE 1 TPC2 messenger RNA expression: quantitative real-time polymerase chain reaction analysis in B16F10 and in B16F0 cells. In basal conditions the primary cell line (B16F0) expresses more TPC2 than the more aggressive (B16F10) sub-line. β-Actin was used as a control. Results represent the mean values of at least three independent experiments ± SEM. Statistical significance: $^{*}p \le .05$, $^{**}p \le .01$, $^{***}p \le .001$. Student's paired *t*-test. SCR versus TPC2-KD B16F0 versus B16F10.

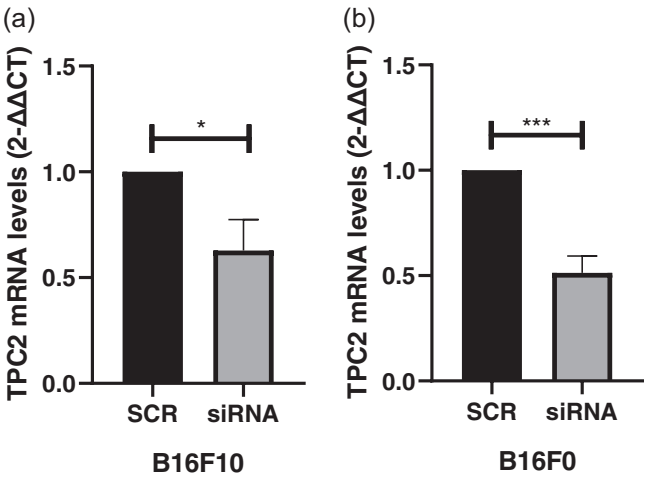

FIGURE 2 TPC2 messenger RNA expression after transient silencing in B16F10 and in B16F0 cells. Quantitative real-time polymerase chain reaction analysis of TPC2 after 24 h of silencing with TPC2 small interfering RNA (siRNA) in B16F10 (a) and B16F0 (b) cells. β-Actin was used as a control. SCR = scrambled control results represent the mean values of at least three independent experiments ± SEM. Statistical significance: $^{*}p \le .05$, $^{**}p \le .01$, $^{***}p \le .001$. Student's paired *t*-test. B16F0SCR versus B16F0 siRNA cell samples and B16F10 SCR versus B16F10 siRNA cell samples.

gene β-actin was used as an internal control to normalise the variability in expression levels. Relative messenger RNA (RNA) expression levels were calculated using the $\Delta\Delta C_T$ method. The sequences of primers used are in Table 1.

2.5 | Flow cytometry analysis

For quantification of m-Cherry TPC2 protein, cells were seeded in 12-culture plates and transfected with the plasmid as previously described. Twenty-four hours after the transfection, the cells were detached by adding 100 µL 0.05% Trypsin-EDTA per well followed by incubation at 37°C for 5 min. Trypsin was inactivated by adding an equal volume of culture medium containing FBS. Un-transfected cells are used to draw negative gates. We used gate for forward (FSC) and side scatter (SSC), then height and area of FSC for a singlet gate, then mCherry fluorescence was analysed using APC (mCherry positive cells are the successfully transfected cells). For cell cycle analysis, the cells were counted after silencing for 24 48, and 72 h, fixed with 70% ethanol, washed three times with phosphate-buffered saline (PBS) and stained for 3 h at room temperature with PI/RNAse, then analysed by flow cytometry (BD FACS Canto™ II Flow Cytometry Systems). Apoptosis was assayed by using PI/Annexin Pacific Blue staining (Thermo Fisher Scientific) and evaluated using flow cytometry.

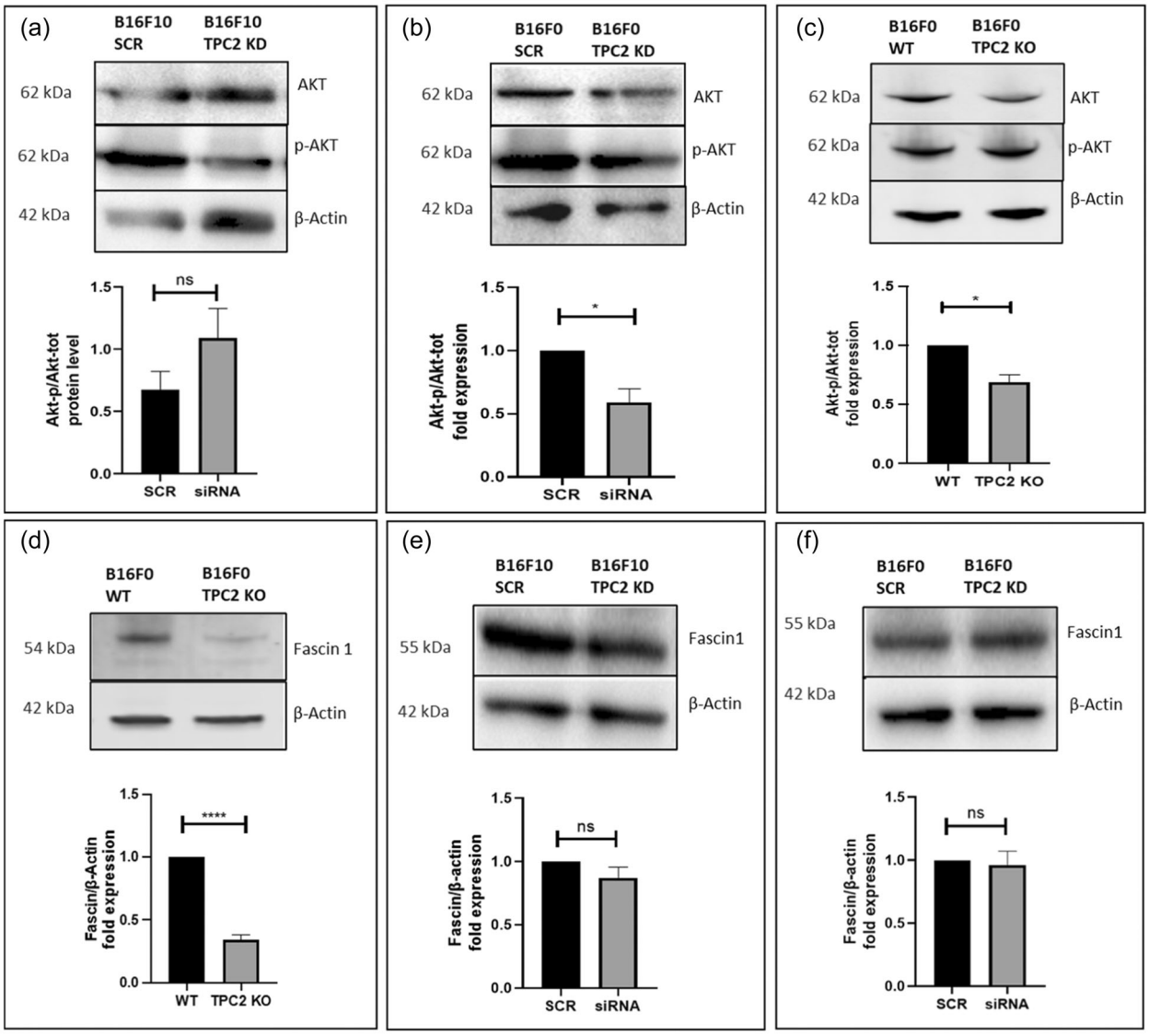

FIGURE 3 AKT activation and Fascin1 expression in the two B16 cell lines. Western blot analysis of: (a) p-AKT/AKT ratio in B16F10 SCR and TPC2-KD cells. (b) p-AKT/AKT ratio in B16F0 scrambled control result (SCR) and TPC2-KD cells. (c) p-AKT/AKT ratio in B16F0 WT and TPC2-KO cells. (d) Fascin1 expression in B16F0 WT and TPC2-KO cells. (e) Fascin1 expression in B16F10 SCR and TPC2-KD samples. (f) Fascin1 expression in B16F0 SCR and TPC2-KD samples. Results represent the mean values of at least three independent experiments ± SEM. Statistical significance: $^*p \le .05$, $^{**}p \le .01$, $^{***}p \le .001$. Student's paired *t*-test. TPC2-SCR versus TPC2-KD and TPC2-WT versus TPC2-KO.

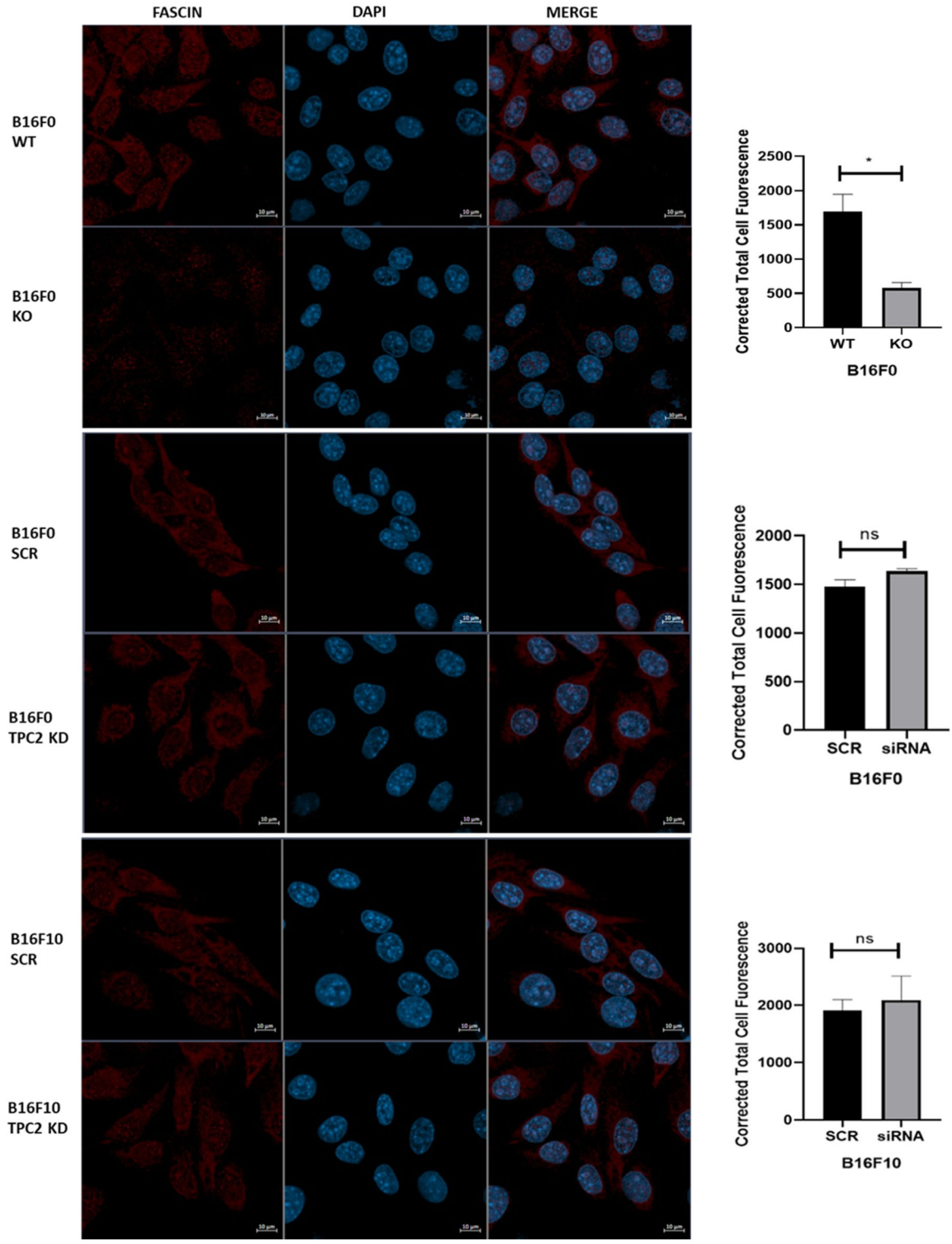

FIGURE 4 Fascin1 immunofluorescence. Fascin 1 was immunolocalized in B16F0 and F10 cells following TPC2 KO (upper panel) and TPC2 KD (medium and lower panels). Dapi nuclear staining. Quantification of Fascin1 fluorescence staining intensity is shown (Mean CTCF values ± SEM). Nuclei are evidenced by 4′,6-diamidino-2-phenylindole blue fluorescence. Results represent the mean values of at least three independent experiments ± SEM. Statistical significance: $^{*}p \leq .05$, $^{**}p \leq .01$ and $^{***}p \leq .001$. Student's paired *t*-test. TPC2-SCR versus TPC2-KD and TPC2-WT versus TPC2-KO.

2.6 | Migration assay

A total of 150,000 cells were seeded in the transwell upper chamber with 1% FBS medium, and 20% FBS medium was added to the bottom chamber. Following 24 h incubation, the cells were removed from the top surface of the membrane. The invasive cells adhering to the bottom surface of the membrane were fixed using 4% paraformaldehyde (Electron Microscopy Sciences) and stained with 600 nM 4′,6-diamidino-2-phenylindole (DAPI) (Thermo Fisher Scientific). The total number of DAPI-stained nuclei of invading cells was counted under a fluorescence microscope by using ImageJ software in five randomly chosen macroscopic fields per membrane. Scratch wound healing assays were performed: briefly, cells were seeded in a 12-well plate with a concentration at 10^5 cells/well. After 24 h, the cells were spread across the plate and a 200 µL micropipette tip was used to scratch through the cells. After washing with PBS, the cells were cultured at 37°C with 5% CO_2 and media. During 24 h, cell migration was photographed with an inverted microscope (×40; Leica).

2.7 | Adhesion assay

Under sterile conditions, 2×10^5 cells were seeded for 90 min on 12-well plates precoated with 10 µg/mL of type1 collagen (c9791; Sigma) at 37°C. After the culture medium was remove

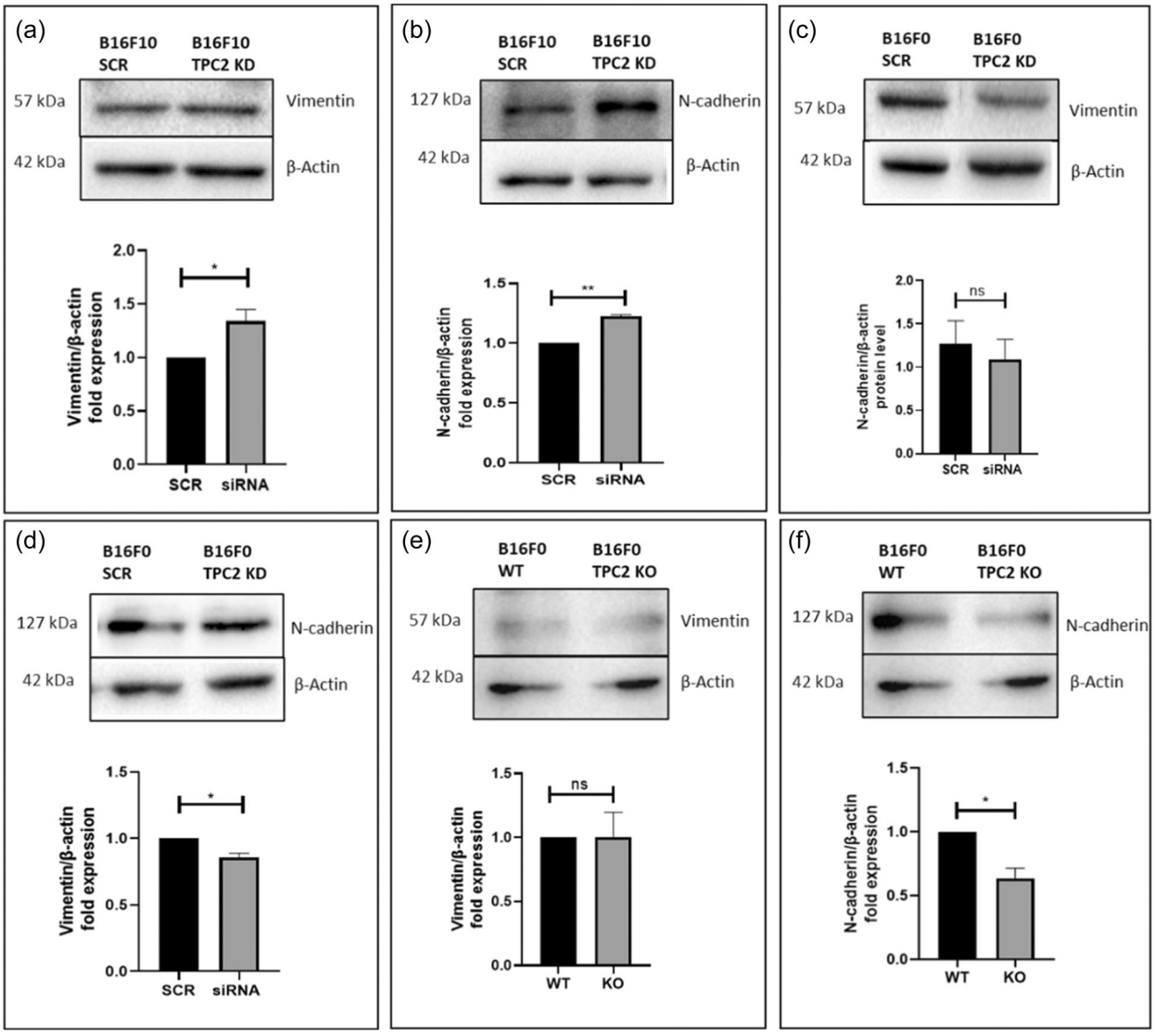

FIGURE 5 Expression of mesenchymal markers vimentin and N-cadherin in TPC2 silenced cells. Western blots. (a, b) TPC2 KD increases the levels of vimentin and N-cadherin in the metastatic subline but (c, d) downregulates vimentin and fails to affect the levels of N-cadherin in the primary cells. (e) Stable genetic silencing (TPC2 KO) of the primary cell line fails to affect vimentin levels but (f) downregulates N-cadherin. Vimentin and N-cadherin levels are normalised to β-actin. Results represent the mean values of at least three independent experiments ± SEM. Statistical significance: $^*p \le .05$, $^{**}p \le .01$ and $^{***}p \le .001$. Student's paired *t*-test. TPC2-SCR versus TPC2-KD and TPC2-WT versus TPC2-KO.

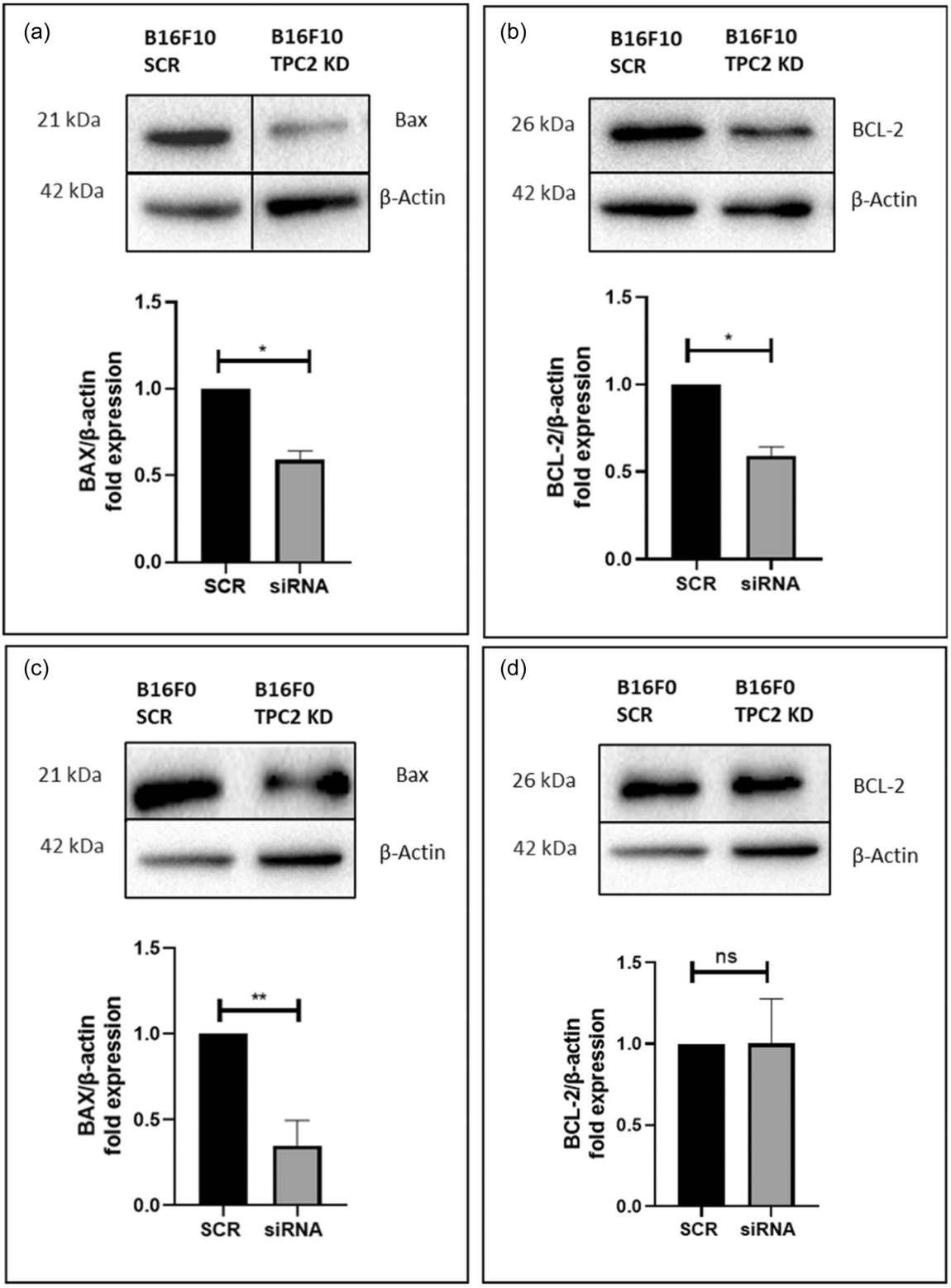

FIGURE 6 Correlation between the expression of TPC2 and apoptosis. (a, b) TPC2 silencing in B16F10 cells downregulates proapoptotic proteins BAX and BCL-2. (c, d) TPC2 silencing downregulates BAX protein in B16F0 cells without significantly changing the expression of BCL-2. (e) No significant percentage of apoptotic cells is present in B16F10 and B16F0 samples (FACS analysis with Annexin V and propidium iodide). Results represent the mean values of at least three independent experiments ± SEM. Statistical significance: $^{*}p \leq .05$, $^{**}p \leq .01$ and $^{***}p \leq .001$. Student's paired *t*-test. TPC2-SCR versus TPC2-KD.

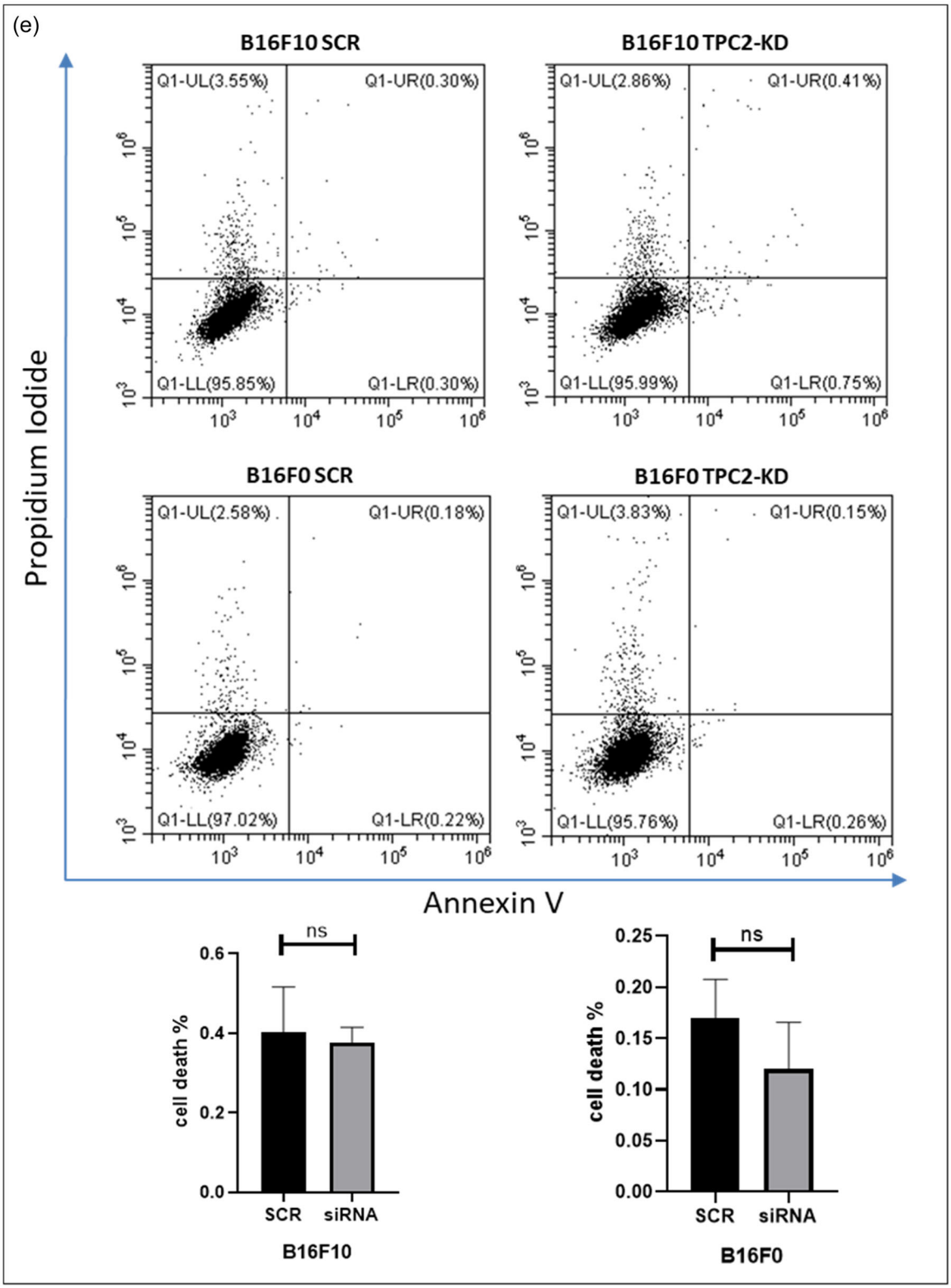

FIGURE 6 (Continued)

the adherent cells were washed with PBS for three times and fixed in 4% paraformaldehyde (Electron Microscopy Sciences) in PBS 10 min at room temperature. The adherent cells were incubated with crystal violet for 30 min at room temperature and after were washed DI water for three times. The plates were left to dry overnight. The next day 10% acetic acid was added to each well to solubilise the crystal violet and the plates were read on a spectrophotometer at 550 nm.

2.8 | Methylthiazolyldiphenyl-tetrazolium (MTT) test

B16F0 and B16F10 cells were silenced for TPC2 and cultured in 96-well plates at a concentration of 1×10^4 cells per well and treated with cisplatin in different concentrations (from 1 to 100 μM) for 24 h. After incubation the medium was removed, 100 μL serum-free medium containing 0.5 mg/mL MTT (m2128; Sigma) solution was added to each well, and the plate was incubated at 37°C for 4 h to allow MTT to be metabolised. Then, 200 μL acid isopropanol 0.04 N was added to each well, pipetting up and down to dissolve crystals, and optical density was read at 550 nm.

2.9 | Immunofluorescence analysis

To analyse B16F0 and B16F10 cell morphological features, cells were cultured for 24 h, in 10% FBS on Ibidi slides (Ibidi, cat. 80826), then silenced for TPC2 and fixed in 4% paraformaldehyde in PBS at 4°C for 10 min. Cells were then permeabilized in PBS 1% BSA/0.1% Triton for 1 h and incubated overnight with mouse anti-Fascin1antibody (1:100 dilution; Santa Cruz). Samples were washed three times in PBS/BSA/Triton for 30 min and incubated with secondary antibody donkey anti-mouse IgG (Donkey anti-Mouse IgG [H + L] Highly Cross-Adsorbed Secondary Antibody, Alexa Fluor™ 546, dil. 1:200). DAPI (600 nM; Thermo Fisher Scientific) was used for nuclei staining. Samples were washed three times in PBS/BSA/Triton for 30 min and covered with glycerol–PBS pH 9.5 for confocal microscopy analysis. Immunofluorescence experiments were analyzed using aZeiss LSM 900 Confocal Microscope. The images were scanned under a ×40 oil immersion objective. Optical spatial series were performed. Quantitative analysis of fluorescence intensity was determined on a maximum projection of each series and quantified as the Corrected Total Cell Fluorescence (CTCF). All analyses were performed using Zeiss Confocal software (Zen 3.0 Blue edition) and ImageJ software.

2.10 | Statistical analysis

Data are presented as the mean ± SEM of results from at least three independent experiments. Student's *t* test was used for statistical comparison between two groups. A value of $p \leq .05$ was considered statistically significant. The data represent the mean ± SEM derived from three independent experiments. $^{*}p < .05$; $^{**}p < .01$ and $^{***}p < .01$. Statistical analysis was performed with GraphPad Prism 8 (GraphPad Software).

3 | RESULTS AND DISCUSSION

3.1 | Comparison of TPC2 expression between B16F0 and B16F10 cells

We have previously shown (D'Amore et al., 2020) that according to the Cancer Genome Atlas, TPC2 (gene name *TPCN2*) exhibits a differential expression between primary and metastatic skin melanoma (SKCM). This difference could indicate a different prognostic role for TPC2 between these two tumour stages, and it is, therefore, important to understand how the expression of TPC2 can influence the course of the disease. To study this issue further we used two murine B16 melanoma cell lines with two different stages of aggressiveness, and first analysed TPC2 gene

TABLE 2 The balance between BAX and BCL-2 determines the resistance (BAX/BCL-2 ratio <1.00) or not to apoptosis.

B16F0				**B16F10**			
Ratio	**BAX/BCL-2**			Ratio	**BAX/BCL-2**		
	BAX	**Arbitrary units**			**BAX**	**Arbitrary units**	
	scr	**siRNA**	**SCR BAX/BCL-2**		**Scr**	**siRNA**	**SCR BAX/BCL-2**
	22.087.125	18.963.024			38.243.673	14.592.773	
	13.643.489	2.882.690			21.845.137	24.983.723	
	5.299.610	11.223.175			40.026.187	29.529.238	
Media	13.676.741	11.022.963	0.765688413	Media	33.371.666	23.035.245	0.627547409
	BCL-2	**Arbitrary units**			**BCL-2**	**Arbitrary units**	
	scr	**siRNA**	**siRNA BAX/BCL-2**		**Scr**	**siRNA**	**siRNA BAX/BCL-2**
	22.386.368	21.360.539			42.131.693	22.549.430	
	19.081.317	19.021.368			41.624.492	18.534.723	
	8.900.711	9.849.054			88.925.291	36.133.643	
Media	16.789.465	16.743.654	0.726275926	Media	57.560.492	25.739.265	0.937436783

Note: BAX and BCL-2 levels were normalised to β-actin.

Abbreviation: siRNA, small interfering RNA.

expression. We observed a decrease in TPC2 messenger RNA (mRNA) expression in cells of B16F10, the metastatic melanoma subline, in comparison with the primary, less aggressive B16F0 cells (Figure 1), which is in line with the patient data set in that both in human and murine melanoma cell lines, the cells with a metastatic phenotype express lower levels of TPC2.

3.2 | TPC2 is differentially expressed in primary and metastatic B16 cells

We have preliminarily analysed the expression of TPC2 in the primary (B16F0) cell line and in its more aggressive sub-line (B16F10) and found that, in line with the data set from human

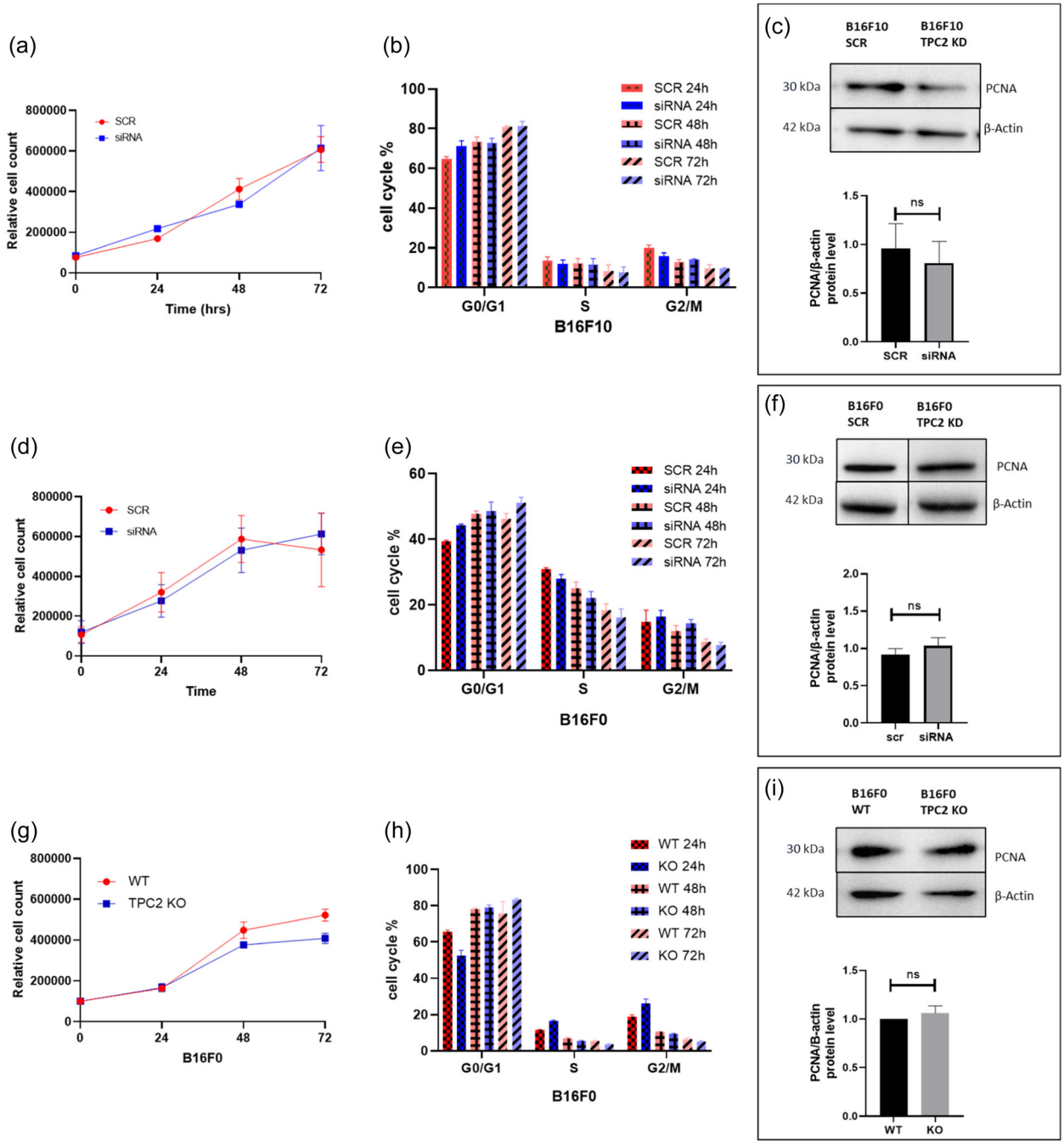

FIGURE 7 Genetic inhibition of TPC2 leaves cell cycle and proliferation rate unaltered in both primary B16F0 and more aggressive B16F10 cells. (a, d, g) Cell counts performed at 24–48–72 h in TPC2-KD and scrambled control in metastatic (B16F10) and primitive (B16F0) cells. (b, e, h) Percentages of cells in G1, S, and G2/M phases at 24–48–72 h: differences between TPC2-SCR and TPC2-KD or between TPC2-WT and TPC2-KO in the metastatic and primitive B16 cell lines. (c, f, i) Western blot analysis showing no differences in PCNA levels following TPC2 KD or KO. PCNA levels normalised to β-actin. Results represent the mean values of at least three independent experiments ± SEM. Statistical significance: $^{*}p \leq .05$, $^{**}p \leq .01$ and $^{***}p \leq .001$. Student's paired *t*-test. TPC2-SCR versus TPC2-KD and TPC2-WT versus TPC2-KO.

melanoma patients (D'Amore et al., 2020), in these murine in vitro models TPC2 is basally expressed at lower levels in the more aggressive cells (Figure 1). To explore whether TPC2, a single gene, can have different functions in different states of neoplastic transformation, we comparatively evaluated how its genetic inhibition can affect these two cell lines that share the same original background but differ in aggressiveness. We performed TPC2 silencing with siRNAs and verified the downregulation of TPC2 (TPC2-KD) after 24 h of culture in B16 F10 (Figure 2a) and B16F0 cells (Figure 2b). The effect of TPC2-KD on a number of biological processes was then comparatively analysed in these cells.

3.3 | Genetic TPC2 inhibition enhances the aggressiveness of the metastatic cells but dampens malignancy traits in the primary cell line

AKT and p-AKT (s473) control the proliferation pathway in several types of cancer, including uveal melanoma (Lago-Baameiro et al., 2023). Recent evidence shows that AKT is constitutively activated in human melanomas and enhances cell survival through NF-κB activation. Immunohistochemical studies of various stages of human melanomas suggest a possible correlation between enhanced AKT activation, tumour progression, and malignancy (Dhawan et al., 2002) indicating AKT as a prognostic marker of melanoma progression. We measured the levels of AKT activation comparing phosphorylated AKT (p-AKT) to total AKT (p-AKT/AKT) in our TPC2-silenced samples and found that TPC2-KD did not affect the p-AKT/AKT ratio in the metastatic B16F10 subline (Figure 3a) but it decreased AKT activation in the primary B16F0 cells (Figure 3b). In line with this latter finding, TPC2-KO in the B16F0 cells also led to a reduction in the p-AKT/AKT ratio (Figure 3c), indicating that TPC2 plays a different role in the two stages of the same malignancy. Ciolczyk-Wierzbicka et al. (2012) have observed that the level of p-AKT is correlated with the level of N-cadherin and the modulation of the cell cycle and proliferation; in our samples the level of N-cadherin is increased in B16F10 TPC2-KD cells, compared to the control. The observation that in the metastatic B16F10 cells TPC2 inhibition increased the levels of the EMT marker N-cadherin while failing to lower p-AKT levels collectively indicate an antitumour role of this channel in this highly aggressive sample. Fascin1 is an actin-binding protein involved in the regulation of cell adhesion and motility. In particular, parallel actin filaments are bundled by Fascin1 in filopodia, lamellipodia, and invadopodia, dynamic protrusions involved in motility and cell interactions. In tumour cells, Fascin1 is expressed in different cancer types and controls extracellular vesicle release, migration and metastasis; the expression of this metastasis-related protein (Liu et al., 2021) was significantly decreased by stable TPC2 inhibition, (TPC2-KO, Figures 3d and 4) in the primary B16F0 cells, but was unaffected by transient TPC2 silencing in all samples (Figures 3e,f and 4). We take this as indicating that the role of TPC2 as a mediator of Fascin1 is indirect, requiring longer inhibition times, possibly related to changes in the deposition of matrix components.

The epithelium-to-mesenchyme transition (EMT) plays a key role in the formation of tumour metastases allowing solid tumours to increase their invasiveness and metastatic activity (Ribatti et al., 2020). Among the molecules recognised as markers of the EMT, N-cadherin and vimentin are upregulated while others, among which is E-cadherin, are downregulated (Ribatti et al., 2020).

Unexpectedly, we found that E-cadherin is not expressed in any of our samples, whether silenced or not for TPC2. TPC2-KD enhanced traits of EMT in B16F10 cells such as an increase in vimentin and N-cadherin expression (Figure 5a,b). Conversely, in

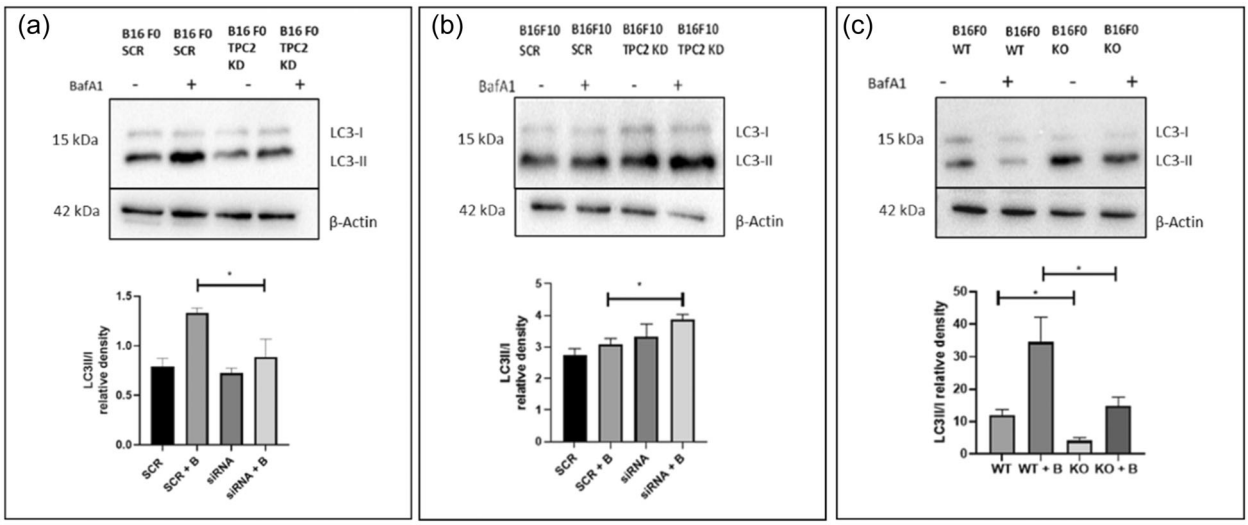

FIGURE 8 Correlation between TPC2 and autophagic flux. Western blot analysis of LC3-II protein in B16F10 and B16F0 cell lines. (a) In B16F10 cells this autophagic marker increases following genetic silencing with TPC2 siRNA. (b, c) Conversely, in B16F0 cells LC3-II decreases in B16F0 TPC2-KD and TPC2-KO cells. LC3-II levels normalised to β-actin. Results represent the mean values of at least three independent experiments ± SEM. Statistical significance: $^{*}p \le .05$, $^{**}p \le .01$, $^{***}p \le .001$. Student's paired *t*-test. SCR versus TPC2-KD; WT versus TPC2-KO. Cells were treated with 1 nM bafilomycin A1 (Baf. A1) to assess the amount of LC3-II protein.

B16F0 cells TPC2-KD resulted in decreased vimentin expression and unchanged N-cadherin expression (Figure 5c,d). In TPC2-KO cells we observed decreased N-cadherin expression (Figure 5e) and unchanged vimentin expression (Figure 5f). The different modulation of vimentin and N-cadherin observed in B16F0 TPC2-KD vs B16F0 TPC2-KO cells could be attributed to the different approaches used for genetic inhibition. Transient silencing could determine the modulation of markers that are not modulated in TPC2-KO (and vice versa), as suggested in a study in which the transient and stable genetic impairment of a single gene were compared (Wang et al., 2018). On the whole, our data on aggressiveness markers confirm that metastatic cells silenced for TPC2 switch to a more mesenchymal and potentially more invasive phenotype while in the primary cells TPC2-KD and TPC2-KO seem to slow down the EMT process.

3.4 | Neither apoptosis nor proliferation are significantly affected by TPC2 inhibition in B16 F0 and F10 cells

The BAX/BCL-2 ratio is based on the expression of two proteins responsible for common mitochondrial apoptosis.

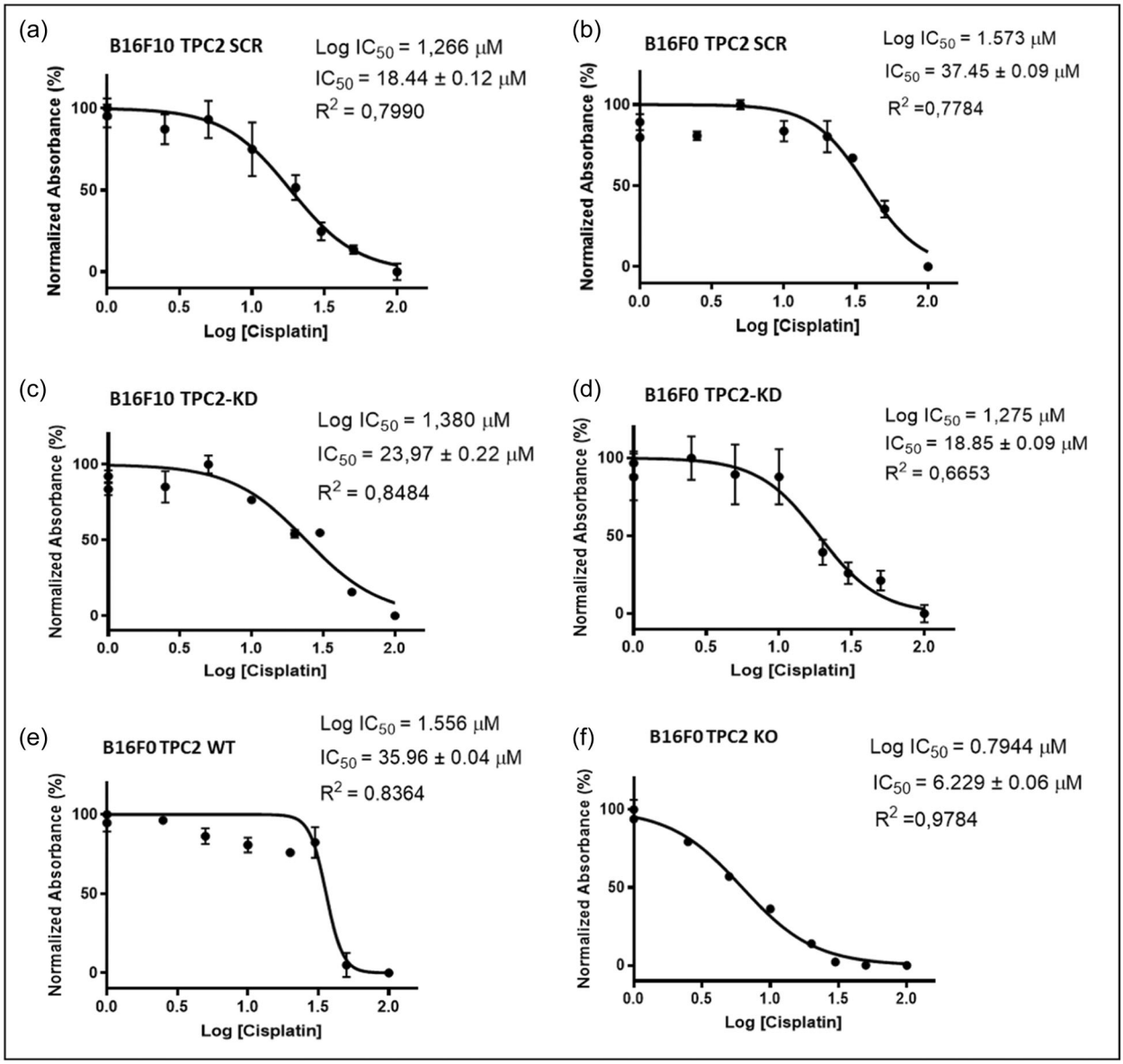

FIGURE 9 Analysis of the sensitivity to cisplatin of cells silenced for TPC2. MTT viability assay: (a–c) The more aggressive cells (B16F10 TPC2-SCR) are substantially more sensitive to cisplatin (IC_{50} = 18.44) than the primary cells (B16F0 TPC2-SCR, IC_{50} = 37.45). Inhibition of TPC2 failed to affect the sensitivity to cisplatin (IC_{50} = 18.85). (b–d) TPC2 silencing in primary cells (B16F0) increased the sensitivity to cisplatin (IC_{50} = 23.97) (IC_{50} = 37.45). (e, f) Primary cells (B16F0) KO for TPC2 created using the CRISPR-CAS9 system are more sensitive to cisplatin than WT cells (IC_{50} = 35.96); the sensitivity of KO cells (IC_{50} = 6.229) appears to be greater than for KD cells (IC_{50} = 23.97). Results represent the mean values of at least three independent experiments ± SEM. Statistical significance: $^{*}p \leq .05$, $^{**}p \leq .01$ and $^{***}p \leq .001$.

B-cell lymphoma protein 2-associated X (BAX) in particular promotes apoptosis, while B-cell lymphoma protein 2 (BCL-2) inhibits it. Their balance can determine, in different tumour contexts, a different prognosis for the patient and the BAX/BCL-2 ratio can be used to predict the course of human melanoma (Raisova et al., 2001). In metastatic melanoma low expression of BAX results in a more favourable prognosis (Guttà et al., 2020), while in the primary tumour low BAX expression correlates with a poorer prognosis. In our TPC2 silenced samples we observed decreased levels of both BAX and BCL-2 proteins in B16F10 cells (Figure 6a,b) while in primary cells (B16F0) TPC2-KD resulted in a similar decrease in BAX levels but BCL-2 levels remained unmodified (Figure 6c,d). In both cases, the ratios, shown in Table 2, are <1.00, as typical of cells resistant to apoptosis. Moreover, no significant percentage of apoptotic cells was found in cytometric analyses (Figure 6e). The proliferative and invasive abilities of malignant cells do not always go hand in hand. We carried out cell counts (Figure 7a,d,g) and analysed the impact of TPC2 expression on the cell cycle of our primary and metastatic cells (Figure 7b,e,h). TPC2 silencing failed to affect proliferation in both cell lines, which was also confirmed by the unaltered levels of the marker proliferating cell nuclear antigen (PCNA) (Figure 7c,f,l). Similarly to apoptosis, proliferation appears therefore independent from TPC2 expression in our experimental models, in agreement with what has been observed in mouse embryonic stem cells (Zhang et al., 2013) silenced for TPC2, and in human melanoma CHL1 TPC2-KO cells compared to the WT samples (D'Amore et al., 2020).

3.5 | Loss of TPC2 increases the autophagic flux of the B16F10 metastatic cell line and reduces it in the B16F0 primary tumour cell line

Recent evidence has shown that the TPC2 channel is often involved in the autophagic process, both in healthy cells and in cancer cells and in the crosstalk between the tumour and the tumour microenvironment (TME) (Sun & Yue, 2018; Wu et al., 2021). We have analysed the autophagic flux in our cell lines silenced for TPC2, using bafilomycin A1 (Baf.A1) which blocks the fusion between the autophagosome and lysosome causing an accumulation of autophagosomes and of autophagic markers, such as LC3-II. Surprisingly, we found that TPC2 plays a dual role in the autophagic process, again dependent on the level of aggressiveness of the cell line analysed. TPC2 inhibition in primary and metastatic cells resulted in opposite changes in LC3-II levels. Namely, in silenced B16F10 metastatic cells LC3-II protein was increased (Figure 8a), while in the primary line B16F0 both TPC2-KD and TPC2-KO resulted in lowered levels of LC3-II (Figure 8b,c). These results suggest a change in the last part of the autophagic process when TPC2 activity or expression is impaired. In contrast, the late steps of the autophagic flux process were upregulated by TPC2 transient silencing in B16F10 cells.

In literature, comparable results have been obtained in different cell types, for example, in cardiomyocytes (García-Rúa et al., 2016) and skeletal muscle (Lin et al., 2015), as well as in Hela or 4T1 (mouse breast tumour cells) (Sun & Yue, 2018), in which TPC2 has been shown to be involved in regulating autophagy. The different behaviour of our two cell populations can be tentatively hypothesised to be due to the more aggressive B16F10 phenotype being less vulnerable than its B16F0 primary counterpart. This point must be taken into consideration when interpreting data from tumour cells since autophagy is a survival mechanism, fundamental in cancer cells subjected to the strong stress imposed by high metabolic and proliferation rates and by the therapies administered to the patient, in which autophagy can be one of the major processes involved in resistance to therapies and immune evasion (Huang et al., 2018; Martin et al., 2017; Yamamoto et al., 2020).

3.6 | Loss of TPC2 affects the resistance of cancer cells to treatment with cisplatin

Recent molecular targeted therapies display strong anticancer efficacy in melanomas carrying the BRAFV600 mutation, while these are ineffective on BRAF wild-type melanomas (Ribas & Flaherty, 2011). A perspective goal for our project, based on BRAF WT cell lines, is to try to discover new potential therapeutic targets that might inhibit tumour growth and metastases. We thus compared the sensitivity to cisplatin of our tumour lines to see possible changes induced by TPC2 silencing in the primary and metastatic cells. Cells were treated with different doses of cisplatin and their viability was checked with an MTT assay (Figure 9 and Table 3). In the more aggressive (B16F10) cells no differences were observed between control and silenced cells (Figure 9a–c). In the primary, B16 F0 cells, on the contrary, TPC2 silencing increased the sensitivity to cisplatin (Figure 9b–d).

TABLE 3 IC_{50} measurements were determined with the MTT viability test (see Materials and Methods), measuring absorbance at 550 nm.

IC50	
B16F10	
SCR	18.44 ± 0.12 μM
TPC2 KD	18.85 ± 0.09 μM
B16F0	
SCR	37.45 ± 0.09 μM
TPC2 KD	23.97 ± 0.22 μM
B16F0	
WT	35.96 ± 0.04 μM
KO	6.229 ± 0.06 μM

3.7 | Silencing of TPC2 increases traits of invasiveness in the metastatic (B16F10) cells but not in the primary (B16F0) cells

The whole of our data suggest that the metastatic phenotype of B16F10 cells is further enhanced by genetic silencing of TPC2, which would represent a novel finding. We next evaluated whether TPC2 siRNA affects the migratory ability of B16F10 cells and found that indeed this was further enhanced in trans well supports (though not in the wound healing assay) (Figure 10a,b). In parallel experiments, adhesion to a collagen type I matrix was tested and showed that TPC2-KD results in decreased binding of B16F10 cells

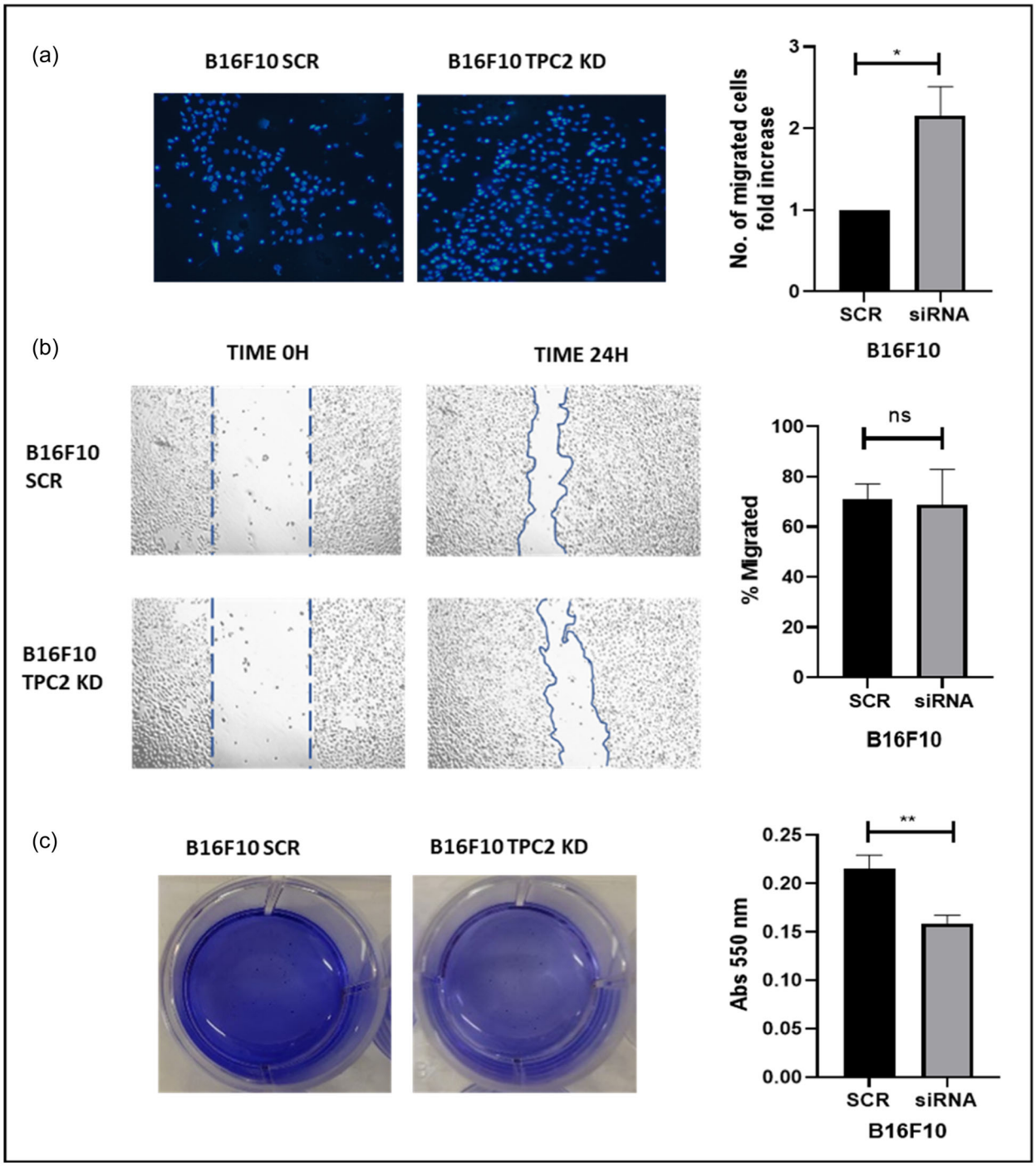

FIGURE 10 TPC2-KD impairs metastatic melanoma cell adhesion to collagen and increases their invasiveness. (a) TPC2 silencing enhances the migration of B16F10 cells apparent in transwell support (4′,6-diamidino-2-phenylindole nuclear-staining) though not (b) in the wound healing assay. (c) Adhesion to type I collagen: TPC2 silencing decreases the adhesiveness of B16F10 cells. Crystal violet staining. Results represent the mean values of at least three independent experiments ± SEM. Statistical significance: $*p \le .05$, $**p \le .01$ and $***p \le .001$. Student's paired *t*-test. SCR versus TPC2-KD.

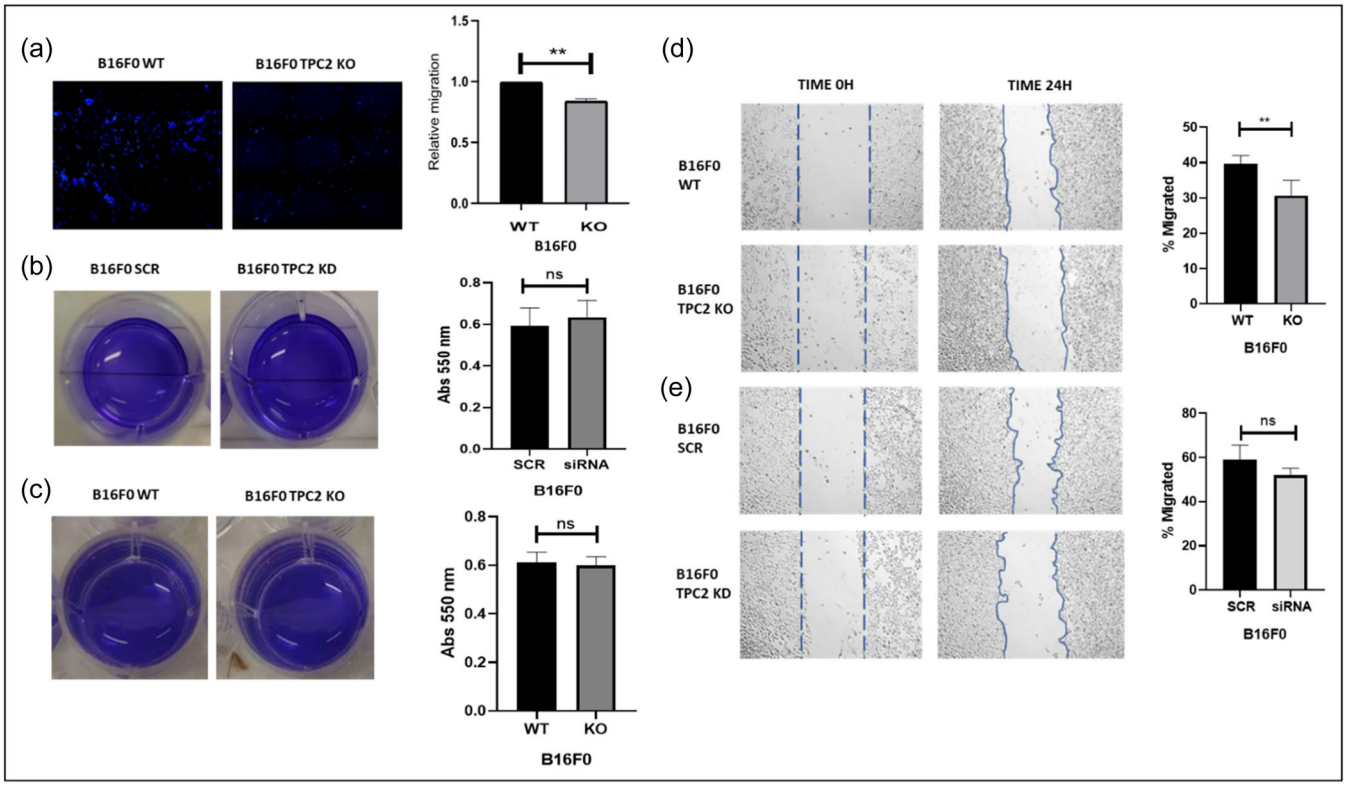

FIGURE 11 Impact of TPC2 impairment on migration and adhesivity in primary (B16F0) samples. (a–d) In B16F0 samples TPC2-KO reduced cell migration in the transwell assay (4′,6-diamidino-2-phenylindole nuclear-staining) and wound healing assay. (e) In B16F0 samples TPC2-KD failed to impair cell migration, as shown in the wound healing assay. (b, c) TPC2-KD and TPC2-KO failed to impair the adhesivity of B16F0 cells to a collagen I matrix (crystal violet stain). Results represent the mean values at the least of three independent experiments ± SEM. Statistical significance: $*p \le .05$, $**p \le .01$, $***p \le .001$; Student's paired *t*-test. SCR versus TPC2-KD or WT versus TPC2-KO.

to this matrix (Figure 10c). The migratory ability of B16F0 cells was analysed following transient and stable TPC2 silencing and was found to be lowered by TPC2-KO (Figure 11a–d) though not by TPC2 KD (Figure 11e). Parallel assays on a collagen type I matrix, showed that silencing of TPC2, either at gene level or transiently, fails to inhibit the adhesion of these primary melanoma cells to a collagen I matrix (Figure 11b,c). Again, loss of TPC2 inactivation differentially affects invasivity traits of the primary cell line and of its metastatic subline. The observation that loss of TPC2 further enhances the migratory phenotype of the metastatic cells is a new finding. In other cell lines, such as murine breast cancer (4T1) and human bladder cancer (T24) cell lines, TPC2 inhibition was reported to reduce the formation of metastasis and impair migration and invasion (Nguyen et al., 2017); analogously, in MNT-1 melanoma cells TPC2-KO results in decreased proliferation and migration (Netcharoensirisuk et al., 2021). Intriguingly, Shivakumar et al. (2017) reported that in bladder cancer the upregulation of TPC2 correlates with an increase in patient survival. The contrasting data regarding the pro- or antitumoural function of TPC2 could be explained by taking into account the heterogeneity of genetic background, tumour types and stage of malignancy (and in the specific case of melanoma, perhaps also the degree of cell pigmentation).

3.8 | Overexpression of TPC2 impairs the migratory ability of B16F10 melanoma cells

To test whether changes in TPC2 expression were directly responsible for the increase in B16F10 metastatic traits, we performed overexpression experiments. Since B16F10 cells express little TPC2 (see Figure 1), we performed a transfection with the TPC2-mCherry plasmid (Ruas et al., 2015), transfection efficiency being evaluated by FACS analysis (Figure 12a), and observed a decrease in the migratory capacity of our cells compared to the control with the empty plasmid and no differences in the adhesion capability between empty and mcherry-TPC2 transfected cells (Figure 12b,c), similar to the results obtained in B16F0 cells silenced or not for TPC2.

4 | CONCLUSIONS

In conclusion, the experimental work described in the present report has addressed the question of whether it is legitimate to attribute an unequivocal pro- or anti-tumoural role to the ion channel TPC2. To our knowledge, this question, posed by discrepancies between some experimental and clinical evidence, has not been explored directly so far, despite the relevance of

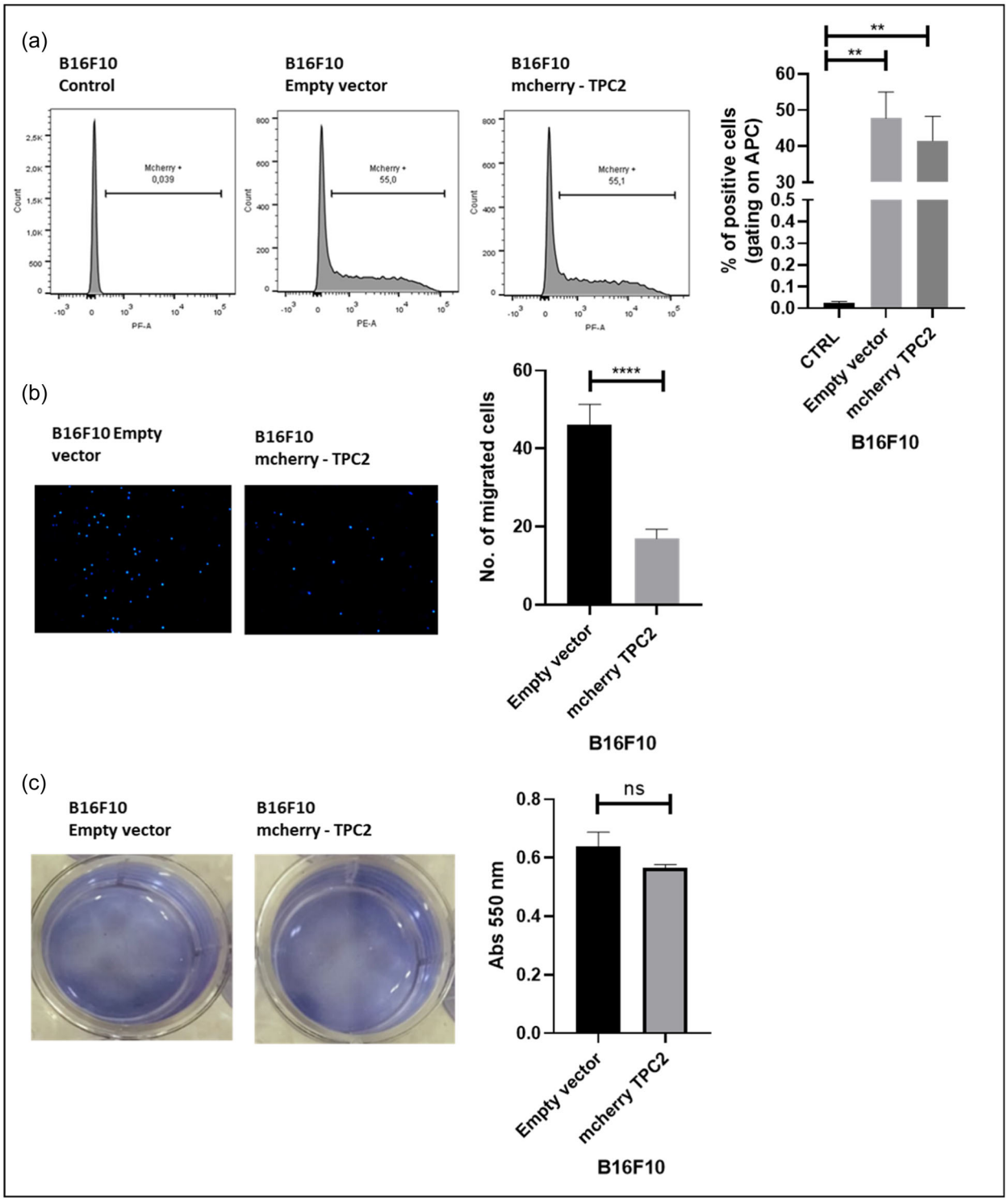

FIGURE 12 Overexpression of TPC2 in the B16F10 highly aggressive cells results in reversion of their migratory ability. (a) FACS analysis of TPC2 overexpression in B16F10. (b) TPC2 overexpression greatly reduces B16F10 cell migration. DAPI nuclear-staining. (c) Overexpression of TPC2 fails to impair the adhesivity of B16F10 cells. Results represent the mean values of at least three independent experiments ± SEM. Statistical significance: $^{*}p \leq .05$, $^{**}p \leq .01$ and $^{***}p \leq .001$. Student's paired *t*-test. Empty vector versus mCherry-TPC2.

TPC2 in pathology and physiology being increasingly recognised. We have reasoned that such a matter could benefit from investigations on a simplified murine experimental in vitro model. As a first approach to our aim, we have focused on melanoma, a malignancy in which TPC2 is known to be differently expressed in the primary versus the late metastatic stages and, to minimise the interference stemming from genetic heterogeneity, we have performed our comparative analysis on cells sharing the same

background but displaying a less versus more aggressive phenotype. The experimental data presented in this article show that in murine B16F10 cells, the metastatic subline of the B16F0 cell line inactivation of TPC2 results in increased aggressiveness, while reducing a number of aggressiveness parameters in the primary cells. Thus, the role of TPC2 in cancer cells appears to be highly dependent not only on the cell type and genetic background, but can also be different/opposite within a single type of malignant cell, according to its stage of tumoural progression. For some time there has been talk of "precision oncology" and "patient-specific therapy" where the main objective is to provide the best therapy against cancer for each patient. This is a very important goal, since we know that while the incidence of melanoma has increased in recent years, the mortality rate has remained stable, thanks to both the prevention that is implemented starting from a young age, and the new therapies in place against this pathology. Yet despite advances in the treatment of melanoma, the development of resistance to treatment in up to 40% of patients (Kozar et al., 2019; Rizos et al., 2014) remains an important clinical problem. It is therefore necessary to study and better understand the mechanisms underlying metastatic melanoma and identify new therapeutic approaches. For this reason, our data, although limited to an in vitro murine model, raise the issue of understanding how far a single gene, silenced in different tumour progression stages, can determine a different tumour phenotype. At present, data obtained using TPC2 inhibitors and activators (Du et al., 2022) together with detailed findings about the TPC2 channel's structure and function, point to TPC2 as being a potential novel druggable target (Jaślan et al., 2023). From the perspective of pharmacologically modulating TPC2 function in malignant melanoma, in vivo experiments and further studies on primitive and metastatic human cell lines will be necessary to extend our findings beyond the limitation of the murine in vitro model used, but our contribution is meant as a starting point, since these kind of comparative investigations could be extended to other primary/metastatic models of human melanoma and of other tumours. This first step could legitimise our initial question and encourage the opening of both an experimental path and a detailed analysis of clinical data. It should be kept in mind that a single molecular target may result in antithetical/opposite biological effects in relation to the stage of tumour progression and when thinking about a potential molecular target for therapy, genetic background and tumour type or level of tumour progression should be taken into account to better define a therapy with 'the right drug, to the right patient and at the right time' (DasGupta et al., 2022).

AUTHOR CONTRIBUTIONS

Samantha Barbonari: Investigation and methodology, formal analysis, writing—original draft. **Antonella D'Amore**: Investigation and methodology. **Ali A. Hanbashi**: Investigation and methodology. **Anna Riccioli**: Methodology and funding acquisition. **Fioretta Palombi**: Conceptualization and validation, writing—review and editing. **Antonio Filippini**: Conceptualization and supervision, project administration and funding acquisition, writing—review and editing. **John Parrington**: Conceptualization and supervision, resources, writing—review and editing. All authors read and approved the final manuscript.

ACKNOWLEDGEMENTS

This research received funding from Ateneo Sapienza University (Ref. Number RG11916B7AF0C02D) for A.R. and (Ref. Number RM12117A8112B2F4; Ref. Number B87G22001200001) A.F.

DATA AVAILABILITY STATEMENT

The data that support the findings of this study are available from the corresponding author upon reasonable request.

All data generated or analyzed during this study are included in this published article.

ETHICS STATEMENT

All authors have read and approved the manuscript, and agreed to submit it to the journal.

ORCID

Samantha Barbonari http://orcid.org/0000-0001-9233-4478
Antonio Filippini https://orcid.org/0000-0001-8453-287X

REFERENCES

Alharbi, A. F., & Parrington, J. (2019). Endolysosomal Ca^{2+} signaling in cancer: The role of TPC2, from tumorigenesis to metastasis. *Frontiers in Cell and Developmental Biology*, *7*, 302. https://doi.org/10.3389/fcell.2019.00302

Alharbi, A. F., & Parrington, J. (2021a). The role of genetic polymorphisms in endolysosomal ion channels TPC2 and P2RX4 in cancer pathogenesis, prognosis, and diagnosis: A genetic association in the UK Biobank. *NPJ Genomic Medicine*, *6*(1), 58. https://doi.org/10.1038/s41525-021-00221-9

Alharbi, A. F., & Parrington, J. (2021b). TPC2 targeting evolution: Leveraging therapeutic opportunities for cancer. *Cell Chemical Biology*, *28*(8), 1103–1105. https://doi.org/10.1016/j.chembiol.2021.07.020

Ambrosio, A. L., Boyle, J. A., Aradi, A. E., Christian, K. A., & Di Pietro, S. M. (2016). TPC2 controls pigmentation by regulating melanosome pH and size. *Proceedings of the National Academy of Sciences*, *113*(20), 5622–5627. https://doi.org/10.1073/pnas.1600108113

Barbonari, S., D'Amore, A., Palombi, F., De Cesaris, P., Parrington, J., Riccioli, A., & Filippini, A. (2022). Relevance of lysosomal Ca(2+) signalling machinery in cancer. *Cell Calcium*, *102*, 102539. https://doi.org/10.1016/j.ceca.2022.102539

Bellono, N. W., Escobar, I. E., & Oancea, E. (2016). A melanosomal two-pore sodium channel regulates pigmentation. *Scientific Reports*, *6*, 26570. https://doi.org/10.1038/srep26570

Chao, Y. K., Chang, S. Y., & Grimm, C. (2023). Endo-lysosomal cation channels and infectious diseases. *Reviews of Physiology Biochemistry and Pharmacology*, *185*, 259–276. https://doi.org/10.1007/112_2020_31

Chao, Y. K., Schludi, V., Chen, C. C., Butz, E., Nguyen, O. N. P., Müller, M., Krüger, J., Kammerbauer, C., Ben-Johny, M., Vollmar, A. M., Berking, C., Biel, M., Wahl-Schott, C. A., &

Grimm, C. (2017). TPC2 polymorphisms associated with a hair pigmentation phenotype in humans result in gain of channel function by independent mechanisms. *Proceedings of the National Academy of Sciences*, *114*(41), E8595–E8602. https://doi.org/10.1073/pnas.1705739114

Chen, C. C., Krogsaeter, E., Kuo, C. Y., Huang, M. C., Chang, S. Y., & Biel, M. (2022). Endolysosomal cation channels point the way towards precision medicine of cancer and infectious diseases. *Biomedicine & Pharmacotherapy*, *148*, 112751. https://doi.org/10.1016/j.biopha.2022.112751

Ciolczyk-Wierzbicka, D., Gil, D., & Laidler, P. (2012). The inhibition of cell proliferation using silencing of N-cadherin gene by siRNA process in human melanoma cell lines. *Current Medicinal Chemistry*, *19*(1), 145–151. https://doi.org/10.2174/092986712803414006

Clementi, N., Scagnolari, C., D'Amore, A., Palombi, F., Criscuolo, E., Frasca, F., Pierangeli, A., Mancini, N., Antonelli, G., Clementi, M., Carpaneto, A., & Filippini, A. (2021). Naringenin is a powerful inhibitor of SARS-CoV-2 infection in vitro. *Pharmacological Research*, *163*, 105255. https://doi.org/10.1016/j.phrs.2020.105255

D'Amore, A., Hanbashi, A. A., Di Agostino, S., Palombi, F., Sacconi, A., Voruganti, A., Taggi, M., Canipari, R., Blandino, G., Parrington, J., & Filippini, A. (2020). Loss of two-pore channel 2 (TPC2) expression increases the metastatic traits of melanoma cells by a mechanism involving the hippo signalling pathway and store-operated calcium entry. *Cancers*, *12*(9), 2391. https://doi.org/10.3390/cancers12092391

DasGupta, R., Yap, A., Yaqing, E. Y., & Chia, S. (2022). Evolution of precision oncology-guided treatment paradigms. *WIREs Mechanisms of Disease*, *15*, e1585. https://doi.org/10.1002/wsbm.1585

Dhawan, P., Singh, A. B., Ellis, D. L., & Richmond, A. (2002). Constitutive activation of akt/protein kinase B in melanoma leads to up-regulation of nuclear factor-kappab and tumor progression. *Cancer Research*, *62*(24), 7335–7342.

Du, C., Guan, X., & Yan, J. (2022). Two-pore channel blockade by phosphoinositide kinase inhibitors YM201636 and PI-103 determined by a histidine residue near pore-entrance. *Communications Biology*, *5*(1), 738. https://doi.org/10.1038/s42003-022-03701-5

Favia, A., Desideri, M., Gambara, G., D'Alessio, A., Ruas, M., Esposito, B., Del Bufalo, D., Parrington, J., Ziparo, E., Palombi, F., Galione, A., & Filippini, A. (2014). VEGF-induced neoangiogenesis is mediated by NAADP and two-pore channel-2–dependent Ca^{2+} signaling. *Proceedings of the National Academy of Sciences*, *111*(44), E4706–E4715. https://doi.org/10.1073/pnas.1406029111

Favia, A., Pafumi, I., Desideri, M., Padula, F., Montesano, C., Passeri, D., Nicoletti, C., Orlandi, A., Del Bufalo, D., Sergi, M., Ziparo, E., Palombi, F., & Filippini, A. (2016). NAADP-Dependent Ca^{2+} signaling controls melanoma progression, metastatic dissemination and neoangiogenesis. *Scientific Reports*, *6*, 18925. https://doi.org/10.1038/srep18925

Ferlay, J., Colombet, M., Soerjomataram, I., Parkin, D. M., Piñeros, M., Znaor, A., & Bray, F. (2021). Cancer statistics for the year 2020: An overview. *International Journal of Cancer*, *149*, 778–789. https://doi.org/10.1002/ijc.33588

García-Rúa, V., Feijóo-Bandín, S., Rodríguez-Penas, D., Mosquera-Leal, A., Abu-Assi, E., Beiras, A., María Seoane, L., Lear, P., Parrington, J., Portolés, M., Roselló-Lletí, E., Rivera, M., Gualillo, O., Parra, V., Hill, J. A., Rothermel, B., González-Juanatey, J. R., & Lago, F. (2016). Endolysosomal two-pore channels regulate autophagy in cardiomyocytes. *The Journal of Physiology*, *594*(11), 3061–3077. https://doi.org/10.1113/JP271332

Geisslinger, F., Müller, M., Chao, Y. K., Grimm, C., Vollmar, A. M., & Bartel, K. (2022). Targeting TPC2 sensitizes acute lymphoblastic leukemia cells to chemotherapeutics by impairing lysosomal function. *Cell Death & Disease*, *13*(8), 668. https://doi.org/10.1038/s41419-022-05105-z

Gerndt, S., Chen, C. C., Chao, Y. K., Yuan, Y., Burgstaller, S., Scotto Rosato, A., Krogsaeter, E., Urban, N., Jacob, K., Nguyen, O. N. P., Miller, M. T., Keller, M., Vollmar, A. M., Gudermann, T., Zierler, S., Schredelseker, J., Schaefer, M., Biel, M., Malli, R., … Grimm, C. (2020). Agonist-mediated switching of ion selectivity in TPC2 differentially promotes lysosomal function. *eLife*, *9*, e54712. https://doi.org/10.7554/eLife.54712

Gunaratne, G. S., Brailoiu, E., He, S., Unterwald, E. M., Patel, S., Slama, J. T., Walseth, T. F., & Marchant, J. S. (2021). Essential requirement for JPT2 in NAADP-evoked Ca^{2+} signaling. *Science Signaling*, *14*(675), eabd5605. https://doi.org/10.1126/scisignal.abd5605

Gunaratne, G. S., Brailoiu, E., Kumar, S., Yuan, Y., Slama, J. T., Walseth, T. F., Patel, S., & Marchant, J. S. (2023). Convergent activation of two-pore channels mediated by the NAADP-binding proteins JPT2 and LSM12. *Science Signaling*, *16*(799), eadg0485. https://doi.org/10.1126/scisignal.adg0485

Gunaratne, G. S., Yang, Y., Li, F., Walseth, T. F., & Marchant, J. S. (2018). NAADP-dependent Ca2+ signaling regulates Middle East respiratory syndrome-coronavirus pseudovirus translocation through the endolysosomal system. *Cell Calcium*, *75*, 30–41. https://doi.org/10.1016/j.ceca.2018.08.003

Guttà, C., Rahman, A., Aura, C., Dynoodt, P., Charles, E. M., Hirschenhahn, E., Joseph, J., Wouters, J., de Chaumont, C., Rafferty, M., Warren, M., van den Oord, J. J., Gallagher, W. M., & Rehm, M. (2020). Low expression of pro-apoptotic proteins Bax, Bak and Smac indicates prolonged progression-free survival in chemotherapy-treated metastatic melanoma. *Cell Death & Disease*, *11*(2), 124. https://doi.org/10.1038/s41419-020-2309-3

Huang, F., Wang, B. R., & Wang, Y. G. (2018). Role of autophagy in tumorigenesis, metastasis, targeted therapy and drug resistance of hepatocellular carcinoma. *World Journal of Gastroenterology*, *24*(41), 4643–4651. https://doi.org/10.3748/wjg.v24.i41.4643

Jaślan, D., Patel, S., & Grimm, C. (2023). New insights into gating mechanisms in TPCs: Relevance for drug discovery. *Cell Calcium*, *112*, 102732. https://doi.org/10.1016/j.ceca.2023.102732

Kondratskyi, A., Kondratska, K., Skryma, R., Klionsky, D. J., & Prevarskaya, N. (2018). Ion channels in the regulation of autophagy. *Autophagy*, *14*(1), 3–21. https://doi.org/10.1080/15548627.2017.1384887

Kozar, I., Margue, C., Rothengatter, S., Haan, C., & Kreis, S. (2019). Many ways to resistance: How melanoma cells evade targeted therapies. *Biochimica et Biophysica Acta (BBA) - Reviews on Cancer*, *1871*(2), 313–322. https://doi.org/10.1016/j.bbcan.2019.02.002

Krogsaeter, E., Rosato, A. S., & Grimm, C. (2022). TRPMLs and TPCs: Targets for lysosomal storage and neurodegenerative disease therapy? *Cell Calcium*, *103*, 102553. https://doi.org/10.1016/j.ceca.2022.102553

Lago-Baameiro, N., Santiago-Varela, M., Camino, T., Silva-Rodríguez, P., Bande, M., Blanco-Teijeiro, M. J., Pardo, M., & Piñeiro, A. (2023). PARK7/DJ-1 inhibition decreases invasion and proliferation of uveal melanoma cells. *Tumori Journal*, *109*(1), 47–53. https://doi.org/10.1177/03008916211061766

Lin, P. H., Duann, P., Komazaki, S., Park, K. H., Li, H., Sun, M., Sermersheim, M., Gumpper, K., Parrington, J., Galione, A., Evans, A. M., Zhu, M. X., & Ma, J. (2015). Lysosomal two-pore channel subtype 2 (TPC2) regulates skeletal muscle autophagic signaling. *The Journal of Biological Chemistry*, *290*(6), 3377–3389. https://doi.org/10.1074/jbc.M114.608471

Lin-Moshier, Y., Keebler, M. V., Hooper, R., Boulware, M. J., Liu, X., Churamani, D., Abood, M. E., Walseth, T. F., Brailoiu, E., Patel, S., & Marchant, J. S. (2014). The two-pore channel (TPC) interactome unmasks isoform-specific roles for TPCs in endolysosomal morphology and cell pigmentation. *Proceedings of the National Academy of*

Sciences, *111*(36), 13087–13092. https://doi.org/10.1073/pnas.1407004111

Liu, H., Zhang, Y., Li, L., Cao, J., Guo, Y., Wu, Y., & Gao, W. (2021). Fascin actin-bundling protein 1 in human cancer: Promising biomarker or therapeutic target? *Molecular Therapy - Oncolytics*, *20*, 240–264. https://doi.org/10.1016/j.omto.2020.12.014

Martin, S., Dudek-Peric, A. M., Garg, A. D., Roose, H., Demirsoy, S., Van Eygen, S., Mertens, F., Vangheluwe, P., Vankelecom, H., & Agostinis, P. (2017). An autophagy-driven pathway of ATP secretion supports the aggressive phenotype of $BRAF^{V600E}$ inhibitor-resistant metastatic melanoma cells. *Autophagy*, *139*, 1512–1527. https://doi.org/10.1080/15548627.2017.1332550

Minicozzi, V., Qi, T., Gradogna, A., Pozzolini, M., Milenkovic, S., Filippini, A., Ceccarelli, M., & Carpaneto, A. (2023). A commentary on the inhibition of human TPC2 channel by the natural flavonoid naringenin: Methods, experiments, and ideas. *Biomolecular Concepts*, *14*(1), 1–6. https://doi.org/10.1515/bmc-2022-0036

Müller, M., Gerndt, S., Chao, Y. K., Zisis, T., Nguyen, O. N. P., Gerwien, A., Urban, N., Müller, C., Gegenfurtner, F. A., Geisslinger, F., Ortler, C., Chen, C. C., Zahler, S., Biel, M., Schaefer, M., Grimm, C., Bracher, F., Vollmar, A. M., & Bartel, K. (2021). Gene editing and synthetically accessible inhibitors reveal role for TPC2 in HCC cell proliferation and tumor growth. *Cell Chemical Biology*, *28*(8), 1119–1131. https://doi.org/10.1016/j.chembiol.2021.01.023

Netcharoensirisuk, P., Abrahamian, C., Tang, R., Chen, C. C., Rosato, A. S., Beyers, W., Chao, Y. K., Filippini, A., Di Pietro, S., Bartel, K., Biel, M., Vollmar, A. M., Umehara, K., De-Eknamkul, W., & Grimm, C. (2021). Flavonoids increase melanin production and reduce proliferation, migration and invasion of melanoma cells by blocking endolysosomal/melanosomal TPC2. *Scientific Reports*, *11*(1), 8515. https://doi.org/10.1038/s41598-021-88196-6

Nguyen, O. N. P., Grimm, C., Schneider, L. S., Chao, Y. K., Atzberger, C., Bartel, K., Watermann, A., Ulrich, M., Mayr, D., Wahl-Schott, C., Biel, M., & Vollmar, A. M. (2017). Two-pore channel function is crucial for the migration of invasive cancer cells. *Cancer Research*, *77*(6), 1427–1438. https://doi.org/10.1158/0008-5472.CAN-16-0852

Nicolson, G. L., Brunson, K. W., & Fidler, I. J. (1978). Specificity of arrest, survival, and growth of selected metastatic variant cell lines. *Cancer Research*, *38*(11 Pt 2), 4105–4111.

Pafumi, I., Festa, M., Papacci, F., Lagostena, L., Giunta, C., Gutla, V., Cornara, L., Favia, A., Palombi, F., Gambale, F., Filippini, A., & Carpaneto, A. (2017). Naringenin impairs two-pore channel 2 activity and inhibits VEGF-induced angiogenesis. *Scientific Reports*, *7*(1), 5121. https://doi.org/10.1038/s41598-017-04974-1

Patel, S., Yuan, Y., Chen, C. C., Jaślan, D., Gunaratne, G., Grimm, C., Rahman, T., & Marchant, J. S. (2022). Electrophysiology of endolysosomal two-pore channels: A current account. *Cells*, *11*(15), 2368. https://doi.org/10.3390/cells11152368

Raisova, M., Hossini, A. M., Eberle, J., Riebeling, C., Wieder, T., Sturm, I., Daniel, P. T., Orfanos, C. E., & Geilen, C. C. (2001). The Bax/Bcl-2 ratio determines the susceptibility of human melanoma cells to CD95/Fas-mediated apoptosis. *The Journal of Investigative Dermatology*, *117*(2), 333–340. https://doi.org/10.1046/j.0022-202x.2001.01409.x

Ribas, A., & Flaherty, K. T. (2011). BRAF-targeted therapy changes the treatment paradigm in melanoma. *Nature Reviews Clinical Oncology*, *8*(7), 426–433. https://doi.org/10.1038/nrclinonc.2011.69

Ribatti, D., Tamma, R., & Annese, T. (2020). Epithelial-mesenchymal transition in cancer: A historical overview. *Translational Oncology*, *13*(6), 100773. https://doi.org/10.1016/j.tranon.2020.100773

Rizos, H., Menzies, A. M., Pupo, G. M., Carlino, M. S., Fung, C., Hyman, J., Haydu, L. E., Mijatov, B., Becker, T. M., Boyd, S. C., Howle, J., Saw, R., Thompson, J. F., Kefford, R. F., Scolyer, R. A., & Long, G. V. (2014). BRAF inhibitor resistance mechanisms in metastatic melanoma: spectrum and clinical impact. *Clinical Cancer Research*, *20*(7), 1965–1977. https://doi.org/10.1158/1078-0432.ccr-13-3122

Roggenkamp, H. G., Khansahib, I., Hernandez C., L. C., Zhang, Y., Lodygin, D., Krüger, A., Gu, F., Möckl, F., Löhndorf, A., Wolters, V., Woike, D., Rosche, A., Bauche, A., Schetelig, D., Werner, R., Schlüter, H., Failla, A. V., Meier, C., Fliegert, R., … Guse, A. H. (2021). HN1L/JPT2: A signaling protein that connects NAADP generation to Ca^{2+} microdomain formation. *Science Signaling*, *14*(675), eabd5647. https://doi.org/10.1126/scisignal.abd5647

Ruas, M., Davis, L. C., Chen, C. C., Morgan, A. J., Chuang, K. T., Walseth, T. F., Grimm, C., Garnham, C., Powell, T., Platt, N., Platt, F. M., Biel, M., Wahl-Schott, C., Parrington, J., & Galione, A. (2015). Expression of Ca2+-permeable two-pore channels rescues-NAADPsignalling inTPC-deficient cells. *The EMBO Journal*, *34*(13), 1743–1758. https://doi.org/10.15252/embj.201490009

Saito, R., Mu, Q., Yuan, Y., Rubio-Alarcón, M., Eznarriaga, M., Zhao, P., Gunaratne, G., Kumar, S., Keller, M., Bracher, F., Grimm, C., Brailoiu, E., Marchant, J. S., Rahman, T., & Patel, S. (2023). Convergent activation of Ca2+ permeability in two-pore channel 2 through distinct molecular routes. *Science Signaling*, *16*(799), eadg0661. https://doi.org/10.1126/scisignal.adg0661

Sakurai, Y., Kolokoltsov, A. A., Chen, C. C., Tidwell, M. W., Bauta, W. E., Klugbauer, N., Grimm, C., Wahl-Schott, C., Biel, M., & Davey, R. A. (2015). Two-pore channels control Ebola virus host cell entry and are drug targets for disease treatment. *Science*, *347*(6225), 995–998. https://doi.org/10.1126/science.1258758

She, J., Zeng, W., Guo, J., Chen, Q., Bai, X., & Jiang, Y. (2019). Structural mechanisms of phospholipid activation of the human TPC2 channel. *eLife*, *8*, e45222. https://doi.org/10.7554/eLife.45222

Shivakumar, M., Lee, Y., Bang, L., Garg, T., Sohn, K. A., & Kim, D. (2017). Identification of epigenetic interactions between miRNA and DNA methylation associated with gene expression as potential prognostic markers in bladder cancer. *BMC Medical Genomics*, *10*(Suppl. 1), 30. https://doi.org/10.1186/s12920-017-0269-y

Skelding, K. A., Barry, D. L., Theron, D. Z., & Lincz, L. F. (2022). Targeting the two-pore channel 2 in cancer progression and metastasis. *Exploration of Targeted Anti-tumor Therapy*, *3*(1), 62–89. https://doi.org/10.37349/etat.2022.00072.

Sun, W., & Yue, J. (2018). TPC2 mediates autophagy progression and extracellular vesicle secretion in cancer cells. *Experimental Cell Research*, *370*(2), 478–489. https://doi.org/10.1016/j.yexcr.2018.07.013

Wang, F., Guo, T., Jiang, H., Li, R., Wang, T., Zeng, N., Dong, G., Zeng, X., Li, D., Xiao, Y., Hu, Q., Chen, W., Xing, X., & Wang, Q. (2018). A comparison of CRISPR/Cas9 and siRNA-mediated ALDH2 gene silencing in human cell lines. *Molecular Genetics and Genomics*, *293*(3), 769–783. https://doi.org/10.1007/s00438-018-1420-y

Webb, S. E., Kelu, J. J., & Miller, A. L. (2020). Role of two-pore channels in embryonic development and cellular differentiation. *Cold Spring Harbor Perspectives in Biology*, *12*(1), a035170. https://doi.org/10.1101/cshperspect.a035170

Wu, Y., Huang, P., & Dong, X. P. (2021). Lysosomal Calcium Channels in Autophagy and Cancer. *Cancers (Basel)*, *13*(6), 1299. https://doi.org/10.3390/cancers13061299

Yamamoto, K., Venida, A., Yano, J., Biancur, D. E., Kakiuchi, M., Gupta, S., Sohn, A. S. W., Mukhopadhyay, S., Lin, E. Y., Parker, S. J., Banh, R. S., Paulo, J. A., Wen, K. W., Debnath, J., Kim, G. E., Mancias, J. D., Fearon, D. T., Perera, R. M., & Kimmelman, A. C. (2020). Autophagy promotes immune evasion of pancreatic cancer by degrading

MHC-I. *Nature*, *581*(7806), 100–105. https://doi.org/10.1038/s41586-020-2229-5

Zhang, Z. H., Lu, Y. Y., & Yue, J. (2013). Two pore channel 2 differentially modulates neural differentiation of mouse embryonic stem cells. *PLoS One*, *8*(6), e66077. https://doi.org/10.1371/journal.pone.0066077

Zhang, J., Guan, X., Shah, K., & Yan, J. (2021). Lsm12 is an NAADP receptor and a two-pore channel regulatory protein required for calcium mobilization from acidic organelles. *Nature Communications*, *12*(1), 4739. https://doi.org/10.1038/s41467-021-24735-z

How to cite this article: Barbonari, S., D'Amore, A., Hanbashi, A. A., Palombi, F., Riccioli, A., Parrington, J., & Filippini, A. (2024). Endolysosomal two-pore channel 2 plays opposing roles in primary and metastatic malignant melanoma cells. *Cell Biology International*, 1–20. https://doi.org/10.1002/cbin.12129